

AD-A150 090

GAIN ENHANCEMENT METHODS FOR PRINTED CIRCUIT ANTENNAS

1/1

(U) CALIFORNIA UNIV LOS ANGELES INTEGRATED


ELECTROMAGNETICS LAB D R JACKSON ET AL. 28 NOV 84

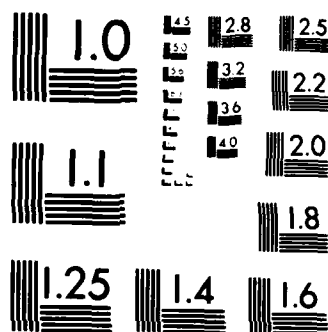
UNCLASSIFIED

UCLA-ENG-84-39 ARO-19778. 5-EL

F/G 9/5

NL

													
								END					
								FORMED					
								OTC					



MICROCOPY RESOLUTION TEST CHART
NATIONAL BUREAU OF STANDARDS 1963-A

UCLA School of Engineering and Applied Science

"Optimization Methods for
Printed Circuit Antennas"

By T.A. Jackson and N.G. Alexopoulos

Sponsored By Research Contract:
F49-620-83-K-0067

Integrated Electromagnetics
Laboratory
Report No. 15
UCLA Report No. ENG-84-39

DTIC
ELECTE
FEB 11 1985

A



DTIC FILE COPY

85 01 29 141

UNCLASSIFIED

SECURITY CLASSIFICATION OF THIS PAGE (When Data Entered)

REPORT DOCUMENTATION PAGE		READ INSTRUCTIONS BEFORE COMPLETING FORM
1. REPORT NUMBER ARO 19778.15-EL	2. GOVT ACCESSION NO. AD-A156696	3. RECIPIENT'S CATALOG NUMBER
4. TITLE (and Subtitle) "Gain Enhancement Methods for Printed Circuit Antennas"		5. TYPE OF REPORT & PERIOD COVERED Technical Report
7. AUTHOR(s) D. R. Jackson and N. G. Alexopoulos		6. PERFORMING ORG. REPORT NUMBER
9. PERFORMING ORGANIZATION NAME AND ADDRESS Electrical Engineering Department UCLA Los Angeles, CA 90024		8. CONTRACT OR GRANT NUMBER(s) U.S. Army DAAG 29-83-K-0067
11. CONTROLLING OFFICE NAME AND ADDRESS U. S. Army Research Office Post Office Box 12211 Research Triangle Park, NC 27709		10. PROGRAM ELEMENT, PROJECT, TASK AREA & WORK UNIT NUMBERS
14. MONITORING AGENCY NAME & ADDRESS (if different from Controlling Office) Army Research Office Research Triangle Park North Carolina		12. REPORT DATE Nov. 28, 1984
		13. NUMBER OF PAGES
		15. SECURITY CLASS. (of this report) Unclassified
		15a. DECLASSIFICATION/DOWNGRADING SCHEDULE
16. DISTRIBUTION STATEMENT (of this Report) Approved for public release; distribution unlimited.		
17. DISTRIBUTION STATEMENT (of the abstract entered in Block 20, if different from Report) NA		
18. SUPPLEMENTARY NOTES The view, opinions, and/or findings contained in this report are those of the author(s) and should not be construed as an official Department of the Army position, policy, or decision, unless so designated by other documentation.		
19. KEY WORDS (Continue on reverse side if necessary and identify by block number)		
20. ABSTRACT (Continue on reverse side if necessary and identify by block number) Resonance conditions for a substrate-superstrate printed antenna geometry which allow for large antenna gain are presented. Asymptotic formulas for gain, beamwidth and bandwidth are presented and the bandwidth limitation of the method is discussed. The method is extended to produce narrow patterns about the horizon, and directive patterns at two different angles.		

UNCLASSIFIED

SECURITY CLASSIFICATION OF THIS PAGE (When Data Entered)

GAIN ENHANCEMENT METHODS FOR PRINTED
CIRCUIT ANTENNAS*

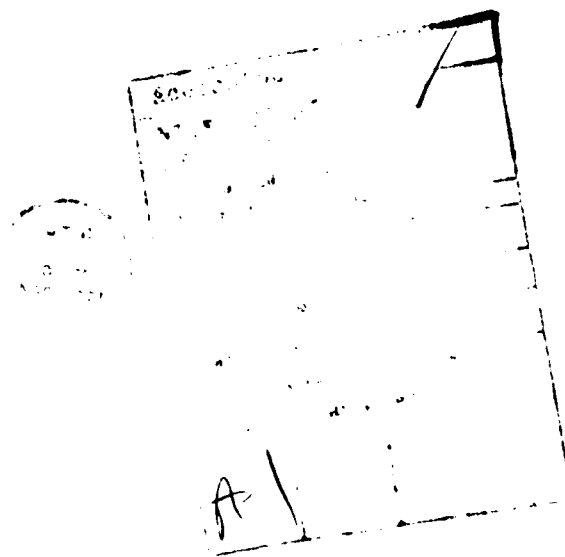
BY

D. R. Jackson and N. G. Alexopoulos
Electrical Engineering Department
University of California Los Angeles
Los Angeles, California 90024

*This research was performed under U.S. Army Research Contract
DAAG 29-83-K-0067.

ABSTRACT

Resonance conditions for a substrate-superstrate printed antenna geometry which allow for large antenna gain are presented. Asymptotic formulas for gain, beamwidth and bandwidth are presented and the bandwidth limitation of the method is discussed. The method is extended to produce narrow patterns about the horizon, and directive patterns at two different angles.



I. INTRODUCTION

It is well documented [1] - [3] that microstrip antennas exhibit many advantages for conformal antenna applications. However, one of the major disadvantages usually associated with printed antennas is low gain. The gain of a typical Hertzian dipole above a grounded substrate is about 6 dB, the gain being relatively insensitive to substrate dielectric constant and thickness for most values typically used in practice. Recently, a method which improves gain significantly for printed antennas was discussed [4] , [5]. This method involves the addition of a superstrate or cover layer over the substrate. It is referred to as Resonance Gain, and it utilizes a superstrate with either $\epsilon \gg 1$ or $\mu \gg 1$. By choosing the layer thicknesses and dipole position properly, a very large gain may be realized at any desired angle θ . The gain varies proportionally to either ϵ or μ , depending on the configuration. However the bandwidth is seen to vary inversely to gain so that a reasonable gain limit is actually established for practical antenna operation. The purpose of this article is to investigate these resonance gain conditions and derive simple asymptotic formulas for resonance gain, beamwidth and bandwidth. The resonance gain condition is then combined with the phenomenon of radiation into the horizon, which results in high gain patterns scanned to the horizon. Finally, the resonance gain condition is extended to produce patterns having resonance gain at more than one angle.

II. RADIATION BY TRANSMISSION LINE ANALOGY

The basic printed antenna geometry under consideration is shown in figure 1. The horizontal Hertzian electric dipole is embedded within a grounded substrate of thickness B having relative permittivity and permeability ϵ_1 , μ_1 . On top of the substrate is the superstrate layer of thickness t

with relative permittivity and permeability ϵ_2, μ_2 . Above the superstrate is free space, with total permittivity and permeability ϵ_0, μ_0 .

A convenient way to analyze the radiation from this antenna structure is by transmission line analogy [4], [7]. In this method the E_x field is determined at the original dipole location due to a Hertzian dipole source in either the $\hat{\theta}$ or $\hat{\phi}$ direction, when the dipole source is far from the origin ($k_0 R \gg 1$) at specified angles θ, ϕ in spherical coordinates. By reciprocity, this must be the E_θ or E_ϕ field at (R, θ, ϕ) due to the original dipole at $z = z_0$. The E_x field near the layered structure due to this reciprocity source is essentially a plane wave, and hence can be accounted for by modeling each layer as a transmission line having a characteristic impedance and propagation constant which depends on the angle θ . The E_θ field corresponds to an \bar{E} field from the reciprocity source which is in the plane of incidence, while the E_ϕ field corresponds to an incident \bar{E} field normal to the plane of incidence. Each case is handled differently by transmission line analogy. The radiated field is obtained to be : (suppressing $e^{+j\omega t}$ time dependence)

$$E_\theta = -\cos\phi \left(\frac{j\omega\mu_0}{4\pi R} \right) e^{-jk_0 R} G(\theta) \quad (1)$$

$$E_\phi = \sin\phi \left(\frac{j\omega\mu_0}{4\pi R} \right) e^{-jk_0 R} F(\theta). \quad (2)$$

The functions $F(\theta)$ and $G(\theta)$ depend on θ only and they represent the voltage (corresponding to \bar{E}_t , the component of the \bar{E} field normal to \hat{z}) at $z = z_0$ in the transmission line analogy due to an incident voltage wave of strength 1 or $\cos\theta$, respectively. The characteristic impedances and propagation constants used in the transmission line analogy are shown in figure 2. The functions $G(\theta)$ and $F(\theta)$ can be written as

$$G(\theta) = 2 \frac{T}{Q + jP} \cos \theta \quad (3)$$

$$F(\theta) = 2 \frac{T}{M + jN} \quad (4)$$

where

$$T = \sin [\beta_1 z_0] \sec[\beta_1 B] \sec[\beta_2 t] \quad (5)$$

$$Q = \tan[\beta_1 B] + \frac{\epsilon_1}{\epsilon_2} \frac{n_2(\theta)}{n_1(\theta)} \tan[\beta_2 t] \quad (6)$$

$$P = - \frac{\epsilon_1}{n_1(\theta)} \cos \theta \left[1 - \frac{\epsilon_2}{\epsilon_1} \frac{n_1(\theta)}{n_2(\theta)} \tan[\beta_1 B] \tan[\beta_2 t] \right] \quad (7)$$

$$M = \tan[\beta_1 B] + \frac{\mu_2}{\mu_1} \frac{n_1(\theta)}{n_2(\theta)} \tan[\beta_2 t] \quad (8)$$

$$N = - \frac{n_1(\theta)}{\mu_1} \sec \theta \left[1 - \frac{\mu_1}{\mu_2} \frac{n_2(\theta)}{n_1(\theta)} \tan [\beta_1 B] \tan[\beta_2 t] \right] \quad (9)$$

with $\beta_1 = k_0 n_1(\theta)$

$$\beta_2 = k_0 n_2(\theta)$$

and

$$n_1(\theta) = \sqrt{n_1^2 - \sin^2 \theta}$$

$$n_2(\theta) = \sqrt{n_2^2 - \sin^2 \theta} \quad .$$

$n_1(\theta)$ and $n_2(\theta)$ represent an effective index of refraction, dependent on the angle θ . These results agree with those obtained by the much more tedious Green's function and stationary phase integration approach for the far field [4]. From (1) and (2) it can be easily shown that the directive gain at angles (θ, ϕ) referred to an isotropic radiator can be expressed as

$$\text{Gain}(\theta, \phi) = \frac{4 \left(\sin^2 \phi |F(\theta)|^2 + \cos^2 \phi |G(\theta)|^2 \right)}{\pi \int_0^{\pi/2} (\sin \theta) \left[|F(\theta)|^2 + |G(\theta)|^2 \right] d\theta} \quad (10)$$

and in dB,

$$\text{Gain}_{\text{dB}}(\theta, \phi) = 10 \log_{10} \text{Gain}(\theta, \phi).$$

In general, the denominator of eq. (10) must be evaluated by numerical integration in order to get the exact gain. However, it is possible to asymptotically evaluate the integral under high gain resonance conditions, leading to a simple formula for the gain.

III. RESONANCE CONDITIONS

There are two types of resonance conditions which exhibit dual kinds of behavior. In the first case, it is required that

$$\frac{n_1 B}{\lambda_0} = \frac{m}{2} \quad (11)$$

$$\frac{n_1 z_0}{\lambda_0} = \frac{2n - 1}{4} \quad (12)$$

and

$$\frac{n_2 t}{\lambda_0} = \frac{2p - 1}{4} \quad (13)$$

where m, n, p are positive integers. Under these conditions, a very high gain pattern is produced at broadside ($\theta = 0$) as the superstrate permittivity becomes large ($\epsilon_2 \gg 1$). In the second case the following conditions must be satisfied:

$$\frac{n_1 B}{\lambda_o} = \frac{2m - 1}{4} \quad (14)$$

$$\frac{n_1 z_o}{\lambda_o} = \frac{2n - 1}{4} \quad (15)$$

and

$$\frac{n_2 t}{\lambda_o} = \frac{2p - 1}{4} \quad (16)$$

When these conditions hold a large gain is obtained at $\theta = 0$ as $\mu_2 \gg 1$. The method requires fairly thick layers, which may be a potential disadvantage for some applications. Taking $m, n, p = 1$ to obtain the thinnest layers possible, it is observed that the dipole is in the middle of the substrate for the type 1 resonance condition, and that the dipole is at the substrate-superstrate interface for the type 2 resonance condition. The second kind of resonance condition allows for a thinner substrate, since (for $m = 1$) $\frac{n_1 B}{\lambda_o} = .25$ instead of .50. However, the second kind of resonance condition may be less practical due to the requirement of a high permeability, low loss superstrate material. Because of this, and the similarity in results, most of this article is devoted to the analysis of type 1 resonance only.

Before any formulas are derived, it may be helpful to present an elementary explanation of the resonance gain phenomenon. With reference to figure 2, the following approximations are obtained for $\theta \ll 1$:

$$Z_{co} = \eta_o$$

$$\beta_o = k_o \left(1 - \frac{1}{2} \theta^2\right)$$

$$Z_{c1} = \eta_o \sqrt{\frac{\mu_1}{\epsilon_1}} \quad \text{and}$$

$$\beta_1 = k_o n_1 \left(1 - \frac{1}{2} \frac{\theta^2}{n_1^2}\right)$$

$$Z_{c2} = \eta_o \sqrt{\frac{\mu_2}{\epsilon_2}}$$

$$\beta_2 = k_o n_2 \left(1 - \frac{1}{2} \frac{\theta^2}{n_2^2}\right) .$$

For the type 1 resonance condition it is required to have $\epsilon_2 \gg 1$ and $k_o n_1 B = m\pi$, $k_o n_2 t = \frac{\pi(2p-1)}{2}$. The input impedance at $z = B$ can thus be written as

$$Z_B = jZ_{c1} \tan[\beta_1 B] \approx -j\eta_o \sqrt{\frac{\mu_1}{\epsilon_1}} \left(2\pi \frac{n_1 B}{\lambda_o}\right) \left(\frac{\theta^2}{2n_1^2}\right)$$

and therefore $Z_B = 0$ for $\theta = 0$. Transmission line #2 acts as a quarter-wave transformer so that the impedance at $z = H$ is given as

$$Z_{in} \approx \frac{Z_{c2}^2}{Z_B} \approx \frac{j\eta_o \left(\frac{\mu_2}{\epsilon_2}\right)}{2\pi \frac{n_1 B}{\lambda_o} \frac{1}{n_1 \epsilon_1} \frac{\theta^2}{2}}$$

and it is noted that $Z_{in} = \infty$ for $\theta = 0$. The voltage at $z = H$ is given by

$$V_{in} = 1 + \Gamma_{in} = \frac{2Z_{in}}{Z_{in} + \eta_o} \quad \text{while the current (corresponding to } \bar{H}_t, \text{ the}$$

component of the \bar{H} field normal to \hat{z}) at $z = B$ is $I_B \approx (-1)^p j \frac{V_{in}}{Z_{c2}}$.

The voltage at $z = z_o$ is then

$$V_o \approx jZ_{c1} I_B \frac{\sin \beta_1 z_o}{\cos \beta_1 B} \\ \approx 2(-1)^{m+n+p+1} \left(\frac{\epsilon_2}{\mu_2} \frac{\mu_1}{\epsilon_1}\right)^{1/2} \left[\frac{1}{1 - j\pi \frac{n_1 B}{\lambda_o} \frac{\epsilon_2}{\mu_2} \frac{1}{n_1 \epsilon_1} \theta^2} \right] .$$

From this result it is noted that when $\theta = 0$, $V_o \propto \sqrt{\epsilon_2}$. For the given antenna configuration, this corresponds to a powerful broadside radiation at $\theta = 0$ in space. Also, defining the angle θ_h at which the voltage at z_o is down by a factor of $1/\sqrt{2}$ from the $\theta = 0$ value, θ_h is obtained as

$$\theta_h \approx 1/\left[\pi \frac{n_1 B}{\lambda_o} \frac{\epsilon_2}{\epsilon_1} \frac{1}{n_1 \mu_2}\right]^{1/2}$$

and therefore $\theta_h \ll 1$ as $\epsilon_2 \gg 1$. This corresponds to an antenna radiation pattern which is highly directive about $\theta = 0$ in space. At $\theta = 0$ the transmission lines act as resonant circuits, hence the name resonance condition. This simple explanation illustrates the fundamental cause of resonance gain. As an illustration of the result, a plot of the \bar{E} - and \bar{H} - plane radiation patterns for a case with $\epsilon_1 = 2.1$, $\epsilon_2 = 100.0$ is shown in figure 3, which involves the lowest mode type 1 resonance condition ($m, n, p = 1$). Figure 4 shows the lowest mode type 2 resonance condition for $\epsilon_1 = 2.1$, $\mu_2 = 100.0$. The patterns in figure 4 look very similar to the ones in figure 3, with the \bar{E} - and \bar{H} - planes interchanged. This dual kind of behavior is always observed between the two types of resonance conditions.

IV. ASYMPTOTIC FORMULAE FOR RESONANCE GAIN, BEAMWIDTH AND BANDWIDTH

As $\epsilon_2 \gg 1$ in the type 1 condition, or $\mu_2 \gg 1$ in the type 2 condition, approximate formulae for the $F(\theta)$ and $G(\theta)$ functions may be obtained near $\theta = 0$ which allow asymptotic formulae for gain, beamwidth and bandwidth to be derived. Because of the length and straightforward nature of the derivation only the results are given here. For $\theta \ll 1$ the approximate forms are:

Case 1 ($\epsilon_2 \gg 1$)

$$|F(\theta)|^2 \approx |G(\theta)|^2 \approx 4 \left(\frac{\epsilon_2}{\epsilon_1} \frac{\mu_1}{\mu_2} \right) \left(\frac{1}{1 + a_1^2 \theta^4} \right) \quad (17)$$

$$\text{with } a_1 = \pi \frac{n_1 B}{\lambda_o} \left(\frac{\epsilon_2}{\epsilon_1} \right) \left(\frac{1}{n_1 \mu_2} \right) \quad (18)$$

Case 2 ($\mu_2 \gg 1$)

$$|F(\theta)|^2 \approx |G(\theta)|^2 \approx 4 \left(\frac{\mu_2}{\epsilon_2} \right) \left(\frac{1}{1 + a_2^2 \theta^4} \right) \quad (19)$$

$$\text{with } a_2 = \pi \frac{n_1 B}{\lambda_o} \frac{\mu_2}{\mu_1} \left(\frac{1}{n_1 \epsilon_2} \right) \quad (20)$$

Defining the beamwidth as $\theta_w = 2\theta_h$ where θ_h is the half-power angle, the gain and beamwidth may be written as

$$\text{Case 1 Gain} \sim 8 \frac{n_1 B}{\lambda_o} \left(\frac{\epsilon_2}{n_1 \epsilon_1 \mu_2} \right) \quad (21)$$

$$\theta_w \sim 2/\sqrt{a_1} \quad \text{as } \epsilon_2 \gg 1 \quad (22)$$

$$\text{Case 2 Gain} \sim 8 \frac{n_1 B}{\lambda_o} \left(\frac{\mu_2}{n_1 \mu_1 \epsilon_2} \right) \quad (23)$$

$$\theta_w \sim 2/\sqrt{a_2} \quad \text{as } \mu_2 \gg 1 \quad (24)$$

In order to discuss bandwidth, approximate formulae are derived for gain which are valid for frequencies close to but not exactly equal to the center frequency f_o (for which equations (11)-(13) or (14)-(16) hold). A frequency

deviation parameter is introduced as

$$\Delta = \frac{f}{f_0} - 1 \quad , \quad (25)$$

measuring the deviation of the normalized frequency. Without presenting the derivation, equations (21) and (23) are modified to become (for $\Delta \ll 1$)

$$\text{Case 1} \quad \text{Gain} \approx 8 \frac{n_1 B}{\lambda_0} \left(\frac{\epsilon_2}{n_1 \epsilon_1 \mu_2} \right) f(b_1 \Delta) \quad (26)$$

$$\text{Case 2} \quad \text{Gain} \approx 8 \frac{n_1 B}{\lambda_0} \left(\frac{\mu_2}{n_1 \mu_1 \epsilon_2} \right) f(b_2 \Delta) \quad (27)$$

where

$$b_1 = 2\pi \frac{n_1 B}{\lambda_0} \frac{\epsilon_2}{\epsilon_1} \frac{n_1}{\mu_2} \quad (28)$$

$$b_2 = 2\pi \frac{n_1 B}{\lambda_0} \frac{\mu_2}{\mu_1} \frac{n_1}{\epsilon_2} \quad (29)$$

and

$$f(x) = \frac{\frac{1}{1+x^2}}{1 + \frac{2}{\pi} \tan^{-1}(x)} \quad (30)$$

The gain formulae are the same as before, except for the function $f(x)$ which determines the frequency behavior of the resonance gain. A graph of $f(x)$ is shown in figure 5. It is noted that $f(0) = 1$ since this represents no frequency deviation. Also, it is interesting to note

that $f(x)$ falls off much more rapidly for $x > 0$ than for $x < 0$. This is due to the fact that for $f < f_0$, the pattern merely broadens as the gain drops. However for $f > f_0$, the pattern broadens slightly and the chief effect is that the pattern is scanned so that the main beam no longer has a peak at $\theta_p = 0$, but rather at

$$\theta_p \approx n_1 \sqrt{2\Delta}, \quad (31)$$

as determined by the condition

$$\frac{n_1 B}{\lambda_0} \sqrt{1 - \sin^2 \theta_p / n_1^2} \approx \left(\frac{n_1 B}{\lambda_0} \right)_{f=f_0} \quad (32)$$

which is a generalization of eqs. (11), (14). This scanning has the effect of reducing more quickly the gain at $\theta = 0$ than the simple pattern broadening does. The directive gain at θ_p remains high, however. More will be said about the results for a scanned beam in the next section. It is observed now that $f(x) = 1/2$ at $x_1 = -2.91$ and $x_2 = +.671$. Hence the bandwidth is determined as

$$\Delta_{w_{1,2}} = \frac{f_2 - f_1}{f_0} \sim \frac{3.58}{b_{1,2}} \quad (33)$$

where f_1 and f_2 are the half-power frequencies, with subscripts 1,2 denoting the type of resonance condition. In order to illustrate the accuracy of the asymptotic formulae for gain, beamwidth and bandwidth, the asymptotic results are compared with the exact solutions in figure 6, with curves shown for some different ϵ_1 values. In order to insure the accuracy

of the asymptotic results it is required that $a_{1,2} \gg 1$ and $b_{1,2} \gg 1$. In practice, for $a_{1,2} \geq 20$ the error in gain will usually be less than 10%.

As can be observed from equations (21) , (23) and (33) the bandwidth is inversely proportional to gain, which sets a limit to achievable gain for practical antenna operation. For example if a bandwidth of at least 5% is desired with a teflon ($\epsilon_1 = 2.1$) substrate, then (from figures 6c,a) $\epsilon_2 \leq 37.0$, and the gain is limited to $\text{Gain} \leq 17.2$ dB.

V. SCANNED MAXIMUM GAIN

The results of the preceeding section can be generalized to the case where the main beam is scanned to an angle $0 < \theta_p < \pi/2$. As already mentioned, this occurs naturally when $f > f_0$ for the cases discussed earlier. In order to create a resonance gain condition at θ_p , equations (11)-(13) or (14)-(16) may be generalized by replacing

$$\frac{n_1 B}{\lambda_0} \quad \text{by} \quad \frac{n_1 B}{\lambda_0} \sqrt{1 - \sin^2 \theta_p / n_1^2} \quad (34)$$

$$\frac{n_1 z_0}{\lambda_0} \quad \text{by} \quad \frac{n_1 z_0}{\lambda_0} \sqrt{1 - \sin^2 \theta_p / n_1^2} \quad (35)$$

and

$$\frac{n_2 t}{\lambda_0} \quad \text{by} \quad \frac{n_2 t}{\lambda_0} \sqrt{1 - \sin^2 \theta_p / n_2^2} \quad (36)$$

The approximate expressions for $F(\theta)$ and $G(\theta)$ about $\theta = \theta_p$ are now fundamentally different than for $\theta_p = 0$. Also, for $\theta_p = 0$ the same

approximate forms resulted for $F(\theta)$ and $G(\theta)$. This is no longer true for $\theta_p > 0$, with the result that the gain is now a function of ϕ as well as the scan angle θ_p . For $0 < \theta_p < \pi/2$ it is found that:

$$|G_{1,2}(\theta)|^2 \approx \frac{|G_{1,2}(\theta_p)|^2}{1 + A_{1,2}^2(\theta - \theta_p)^2} \quad (37)$$

and

$$|F_{1,2}(\theta)|^2 \approx \frac{|F_{1,2}(\theta_p)|^2}{1 + B_{1,2}^2(\theta - \theta_p)^2} \quad (38)$$

where

Case 1 $|G_1(\theta_p)|^2 \approx 4 \left(\frac{\epsilon_2}{\epsilon_1} \frac{\mu_1}{\mu_2} \right) (\cos^2 \theta_p) \left(1 - \sin^2 \theta_p / n_1^2 \right)$ (39)

$$|F_1(\theta_p)|^2 \approx 4 \left(\frac{\epsilon_2}{\epsilon_1} \frac{\mu_1}{\mu_2} \right) \left(1 - \sin^2 \theta_p / n_1^2 \right)^{-1} \quad (40)$$

$$A_1 = 2\pi \frac{n_1 B}{\lambda_o} \frac{\epsilon_2}{\mu_2} \frac{1}{n_1 \epsilon_1} \sin \theta_p \cos^2 \theta_p \quad (41)$$

$$B_1 = 2\pi \frac{n_1 B}{\lambda_o} \frac{\epsilon_2}{\mu_2} \frac{1}{n_1 \epsilon_1} \sin \theta_p \left(1 - \sin^2 \theta_p / n_1^2 \right)^{-1} \quad (42)$$

Case 2 $|G_2(\theta_p)|^2 \approx 4 \left(\frac{\mu_2}{\epsilon_2} \right)$ (43)

$$|F_2(\theta_p)|^2 \approx 4 \left(\frac{\mu_2}{\epsilon_2} \right) \cos^2 \theta_p \quad (44)$$

$$A_2 = 2\pi \frac{n_1 B}{\lambda_o} \frac{\mu_2}{\epsilon_2} \frac{1}{n_1 \mu_1} \sin \theta_p \left(1 - \sin^2 \theta_p / n_1^2\right)^{-1} \quad (45)$$

$$B_2 = 2\pi \frac{n_1 B}{\lambda_o} \frac{\mu_2}{\epsilon_2} \frac{1}{n_1 \mu_1} \sin \theta_p \cos^2 \theta_p \quad (46)$$

and therefore gain is now given by the expression

$$\text{Gain}_{1,2}(\theta_p, \phi) \sim \frac{4 \left(\sin^2 \phi |F_{1,2}(\theta_p)|^2 + \cos^2 \phi |G_{1,2}(\theta_p)|^2 \right)}{(\sin \theta_p) \left[\frac{|F_{1,2}(\theta_p)|^2}{B_{1,2}} \zeta(B_{1,2}) + \frac{|G_{1,2}(\theta_p)|^2}{A_{1,2}} \zeta(A_{1,2}) \right]} \quad (47)$$

$$\text{where } \zeta(x) = \tan^{-1} [x(\pi/2 - \theta_p)] + \tan^{-1} [x\theta_p]. \quad (48)$$

The beamwidths in the principle planes are now found to be:

E - Plane ($\phi = 0$)

$$\theta_{w1,2} \sim \frac{2}{A_{1,2}} \quad (49)$$

H - Plane ($\phi = \pi/2$)

$$\theta_{w1,2} \sim \frac{2}{B_{1,2}} \quad (50)$$

In addition the bandwidth can be written as

$$\Delta_{w1,2} \sim \theta_{w1,2} \left[\frac{\sin \theta_p \cos \theta_p}{n_1^2 - \sin^2 \theta_p} \right] \quad (51)$$

where the term in brackets determines the shift in normalized frequency f/f_0 required to produce a small shift in θ_p .

Plots showing a comparison of the asymptotic and exact results for gain, beamwidth and bandwidth for $\epsilon_1 = 2.1$ (teflon) for different scan angles are shown in figures 7 - 9. For accurate asymptotic results it is required that

$$A_{1,2} \geq 10 \text{ and } B_{1,2} \geq 10,$$

which insures an error of less than 10% for the gain curves shown.

Of interest is the fact that \bar{E} - Plane gain decreases for increasing θ_p while \bar{H} - Plane gain increases. A pattern for type 1 resonance gain scanned to $\theta_p = 45^\circ$ is shown in figure 10, for $\epsilon_2 = 100.0$.

VI. RESONANT RADIATION INTO THE HORIZON

The approximate expressions for $G(\theta)$ and $F(\theta)$ for scanned resonance, equations (37) and (38), are only valid for $\theta_p < \pi/2$. It is not always possible to produce a pattern which is scanned to the horizon ($\theta_p = \pi/2$) because in general the radiation from a printed antenna always tends to zero as $\theta \rightarrow \frac{\pi}{2}$. An exception to this occurs when a TE or TM mode is exactly at cutoff. When a TE mode is at cutoff, the $F(\theta)$ function remains non zero as $\theta \rightarrow \pi/2$, and when a TM mode is at cutoff the $G(\theta)$ function remains non zero as $\theta \rightarrow \pi/2$. This phenomenon, called radiation into the horizon, is discussed in [6]. The superstrate thickness required for mode cutoff is given by [6]

TE Mode

$$\frac{n_2 t}{\lambda_0} = \frac{n_2}{2\pi\sqrt{n_2^2 - 1}} \tan^{-1} \left[\frac{\mu_2}{\mu_1} \frac{\sqrt{n_1^2 - 1}}{\sqrt{n_2^2 - 1}} \cot \left(2\pi \frac{n_1 B}{\lambda_0} \sqrt{1 - 1/n_1^2} \right) \right] \quad (52)$$

TM Mode

$$\frac{n_2 t}{\lambda_0} = \frac{n_2}{2\pi \sqrt{n_2^2 - 1}} \tan^{-1} \left[-\frac{\epsilon_2}{\epsilon_1} \frac{\sqrt{n_1^2 - 1}}{\sqrt{n_2^2 - 1}} \tan \left(2\pi \frac{n_1 B}{\lambda_0} \sqrt{1 - 1/n_1^2} \right) \right] \quad (53)$$

If it is assumed that

$$\frac{n_1 B}{\lambda_0} \sqrt{1 - 1/n_1^2} = \frac{m}{2} \quad (54)$$

which gives the substrate thickness for scanning to $\theta_p = \pi/2$ for the type 1 resonance condition, then from (52) the result

$$\frac{n_2 t}{\lambda_0} = \frac{\frac{2p - 1}{4}}{\sqrt{1 - 1/n_2^2}} \quad (55)$$

is obtained, which is the same thickness required for resonance radiation at $\theta_p = \pi/2$ as given by eqs. (13) and (36). Hence the phenomena of resonance gain and radiation into the horizon can be combined for the \bar{H} - Plane pattern, which is determined by the $F(\theta)$ function. Similarly, if for the type 2 resonance condition the relationship

$$\frac{n_1 B}{\lambda_0} \sqrt{1 - 1/n_1^2} = \frac{2m - 1}{4} \quad (56)$$

is satisfied, then eq. (53) yields the result given by eq. (55). Hence \bar{E} - Plane resonant radiation into the horizon for the type 2 resonance condition can be obtained. A pattern illustrating \bar{H} - Plane resonant

radiation into the horizon is shown in figure 11. The radiation pattern is narrow about the horizon in the \bar{H} - Plane. The \bar{E} - Plane pattern tends to zero at the horizon, since radiation into the horizon is only occurring for the E_ϕ field (TE mode cutoff) here.

For resonant radiation into the horizon the approximate forms for $\theta \approx \pi/2$ are

$$\text{Case 1} \quad |F(\theta)|^2 \approx \frac{|F(\pi/2)|^2}{1 + E^2(\theta - \pi/2)^2} \quad (57)$$

$$\text{Case 2} \quad |G(\theta)|^2 \approx \frac{|G(\pi/2)|^2}{1 + F^2(\theta - \pi/2)^2} \quad (58)$$

$$\text{where} \quad |F(\pi/2)|^2 = 4 \left(\frac{\epsilon_2}{\epsilon_1} \frac{\mu_1}{\mu_2} \right) \frac{1}{1 - 1/n_1^2} \quad (59)$$

$$|G(\pi/2)|^2 = 4 \left(\frac{\mu_2}{\epsilon_2} \right) \quad (60)$$

$$\text{and} \quad E = \pi \frac{n_1 B}{\lambda_o} \left(\frac{\epsilon_2}{\mu_2} \frac{1}{n_1 \epsilon_1} \frac{1}{1 - 1/n_1^2} \right) \quad (61)$$

$$F = \pi \frac{n_1 B}{\lambda_o} \left(\frac{\mu_2}{\epsilon_2} \frac{1}{n_1 \mu_1} \frac{1}{1 - 1/n_1^2} \right) \quad (62)$$

Unfortunately, asymptotic expressions for $G(\theta)$ for Case 1 or $F(\theta)$ for Case 2 are not easy to obtain, and thus no asymptotic formulae for the gain can be presented. The beamwidths in the principle planes of resonant radiation are found from equations (57) and (58) in a straightforward manner as before, however. Additionally, it is not possible to define

bandwidth in a meaningful way as before, since radiation into the horizon only occurs for the frequency corresponding to mode cutoff. A bandwidth definition for radiation into the horizon is discussed in [6].

VII. SCANNING FOR MULTIPLE ANGLES

As an extension of scanning the beam to θ_p , the substrate thickness and refractive index can be chosen so as to allow for resonant gain scanning at two different angles θ_1 and θ_2 . For the type 1 condition,

$$\frac{n_1 B}{\lambda_o} \sqrt{1 - \sin^2 \theta_1 / n_1^2} = \frac{m}{2} \quad (63)$$

$$\frac{n_1 B}{\lambda_o} \sqrt{1 - \sin^2 \theta_2 / n_1^2} = \frac{n}{2} \quad (64)$$

and

$$\frac{n_1 z_o}{\lambda_o} \sqrt{1 - \sin^2 \theta_1 / n_1^2} = \frac{2p - 1}{4} \quad (65)$$

$$\frac{n_1 z_o}{\lambda_o} \sqrt{1 - \sin^2 \theta_2 / n_1^2} = \frac{2q - 1}{4} \quad (66)$$

must be satisfied. Assuming $\theta_1 < \theta_2$, it follows that $n < m$ and $q < p$.

Furthermore

$$\frac{n}{m} = \frac{2q - 1}{2p - 1} > \sqrt{\frac{1 - \sin^2 \theta_2}{1 - \sin^2 \theta_1}} \quad (67)$$

since $n_1, n_2 \geq 1$. The integers m and n may be chosen for the thinnest possible substrate, which makes them odd. p and q may then be determined from $m = 2p - 1$ and $n = 2q - 1$. The superstrate thickness can be set from eq. (13).

It therefore follows that

$$n_1^2 = \frac{\sin^2 \theta_2 - \left(\frac{n}{m}\right)^2 \sin^2 \theta_1}{1 - \left(\frac{n}{m}\right)^2} \quad (68)$$

and

$$\frac{n_1 B}{\lambda_o} = \frac{m/2}{\sqrt{1 - \sin^2 \theta_1 / n_1^2}} \quad (69)$$

For the type 2 resonance condition equation (68) must be satisfied with

$$\frac{n_1 B}{\lambda_o} = \frac{m/4}{\sqrt{1 - \sin^2 \theta_1 / n_1^2}} \quad (70)$$

To avoid any additional resonances other than the ones at θ_1 and θ_2 the following criteria should be satisfied:

$$m = n + 2 \quad (71)$$

$$\frac{n_1 B}{\lambda_o} \sqrt{1 - 1/n_1^2} > \frac{n - 2}{2} \quad (72)$$

and

$$\frac{n_1 B}{\lambda_o} < \frac{m + 2}{2} \quad (73)$$

This places a restriction on how close together θ_1 and θ_2 may be. For example, using $n = 3$, $m = 5$ and choosing $\theta_1 = 30^\circ$, equation (72) yields the restriction $\theta_2 > 60^\circ$.

As an example, if θ_1 and θ_2 are chosen as $\theta_1 = 30^\circ$ and $\theta_2 = 70^\circ$, m and n must satisfy

$$\frac{n}{m} \geq .39493 \quad (\text{from eq. 67}).$$

Choosing

$n = 3$, $m = 5$ (for the thinnest possible substrate) there results
(with $\mu_1 = 1.0$)

$$n_1^2 = \epsilon_1 = 1.23910$$

and

$$\frac{n_1 B}{\lambda_0} = 2.79816.$$

The \bar{E} - and \bar{H} - Plane patterns for this case are shown in figure 12 for $\epsilon_2 = 25.0$. Both \bar{E} - and \bar{H} - Plane patterns are seen to be highly directive about $\theta = 30^\circ$ and 70° . There are no other resonances here since equations (71)-(73) are satisfied.

VIII. CONCLUSION

Two dual types of resonance conditions have been established for a substrate-superstrate antenna geometry which allow for large antenna gain as the ϵ or μ of the superstrate becomes large in the respective cases. For these resonance conditions the gain is proportional to the ϵ or μ of the superstrate and therefore large gains may be obtained. The bandwidth is inversely proportional to the gain, however, so a practical limit is set for normal antenna operation. Asymptotic formulas for gain, beamwidth and bandwidth have been presented for the cases of broadside radiation and for scanning to an arbitrary angle θ_p for $0 < \theta_p < \pi/2$. Resonance gain is observed to combine with the phenomenon of radiation into the horizon in order to create patterns which are narrow about the horizon. Finally, it is shown that resonance gain can be produced at two different angles, but the substrate refractive index is then no longer arbitrary.

REFERENCES

- [1] I. J. Bahl and P. Bhartia, Microstrip Antennas, Artech House, Inc., Dedham MA, 1980.
- [2] J. R. James, P. S. Hall, and C. Wood, Microstrip Antenna Theory and Design, Peter Peregrinus, Ltd., 1981, IEE Electromagnetic Waves Series 12.
- [3] K. R. Carver and J. W. Mink, "Microstrip Antenna Technology", IEEE Trans. Antennas Propagat., vol. AP-29, No. 1, pp. 2-24, Jan. 1981.
- [4] N. G. Alexopoulos and D. R. Jackson, "Fundamental Superstrate (Cover) Effects on Printed Circuit Antennas", IEEE Trans. Antennas Propagat., vol. AP-32, pp. 807-816, Aug. 1984.
- [5] Y. Sugio, T. Makimoto, S. Nishimura, and H. Nakanishi, "Analysis for Gain Enhancement of Multiple-Reflection Line Antenna with Dielectric Plates", Trans. IECE, pp. 80-112, Jan. 1981.
- [6] N. G. Alexopoulos, D. R. Jackson, and P. B. Katehi, "Criteria for Nearly Omnidirectional Radiation Patterns for Printed Antennas", UCLA Report No. ENG-84-13, May 1984. Accepted for publication, IEEE Trans. Antennas Propagat.
- [7] Ramo, Whinnery, and Van Duzer, "Fields and Waves in Communication Electronics", Third Edition, Ch. 6, John Wiley, New York, 1965.

ACKNOWLEDGEMENTS. The authors wish to thank Ms. M. Schoneberg for typing the manuscript.

FIGURE CAP TIONS

- Figure 1 - Superstrate-substrate geometry
- Figure 2 - Transmission line analogy
- Figure 3a - \bar{E} -plane pattern for type 1 resonance condition
- Figure 3b - \bar{H} -plane pattern for type 1 resonance condition
- Figure 4a - \bar{E} -plane pattern for type 2 resonance condition
- Figure 4b - \bar{H} -plane pattern for type 2 resonance condition
- Figure 5 - Bandwidth function $f(x)$
- Figure 6a - Resonance gain vs. ϵ_2
- Figure 6b - Resonance beamwidth vs. ϵ_2
- Figure 6c - Resonance bandwidth vs. ϵ_2
- Figure 7a - \bar{E} -plane resonance gain vs. ϵ_2 for different scan angles
- Figure 7b - \bar{H} -plane resonance gain vs. ϵ_2 for different scan angles
- Figure 8a - \bar{E} -plane resonance beamwidth vs. ϵ_2 for different scan angles
- Figure 8b - \bar{H} -plane resonance beamwidth vs. ϵ_2 for different scan angles
- Figure 9a - \bar{E} -plane resonance bandwidth vs. ϵ_2 for different scan angles
- Figure 9b - \bar{H} -plane resonance bandwidth vs. ϵ_2 for different scan angles
- Figure 10a - \bar{E} -plane pattern for $\theta_p = 45^\circ$
- Figure 10b - \bar{H} -plane pattern for $\theta_p = 45^\circ$
- Figure 11a - \bar{H} -plane pattern for \bar{H} -plane resonant radiation into the horizon
- Figure 11b - \bar{E} -plane pattern for \bar{H} -plane resonant radiation into the horizon
- Figure 12a - \bar{E} -plane pattern for $\theta_1 = 30^\circ$, $\theta_2 = 70^\circ$
- Figure 12b - \bar{H} -plane pattern for $\theta_1 = 30^\circ$, $\theta_2 = 70^\circ$

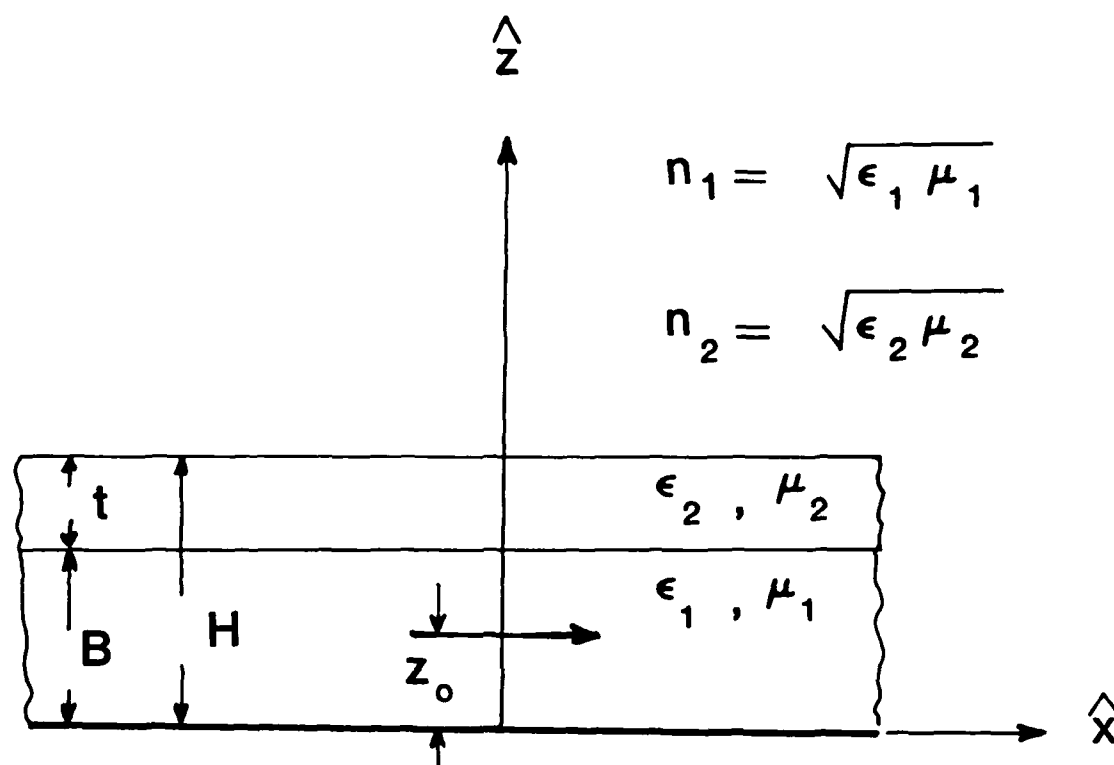
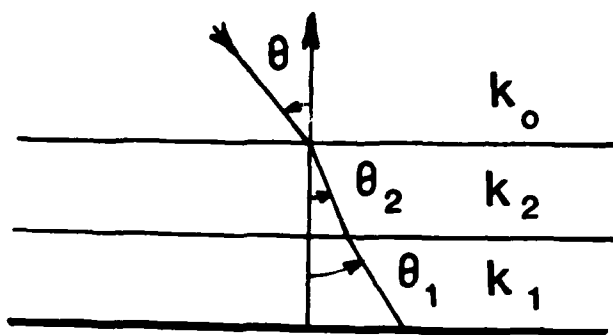


Figure 1

Superstrate - Substrate Geometry



$$n_1(\theta) = n_1 \cos(\theta_1) = \sqrt{n_1^2 - \sin^2(\theta)}$$

$$n_2(\theta) = n_2 \cos(\theta_2) = \sqrt{n_2^2 - \sin^2(\theta)}$$

For F(θ)

$$Z_{co} = \eta_o \sec(\theta)$$

$$Z_{c1} = \eta_o \mu_1 / n_1(\theta)$$

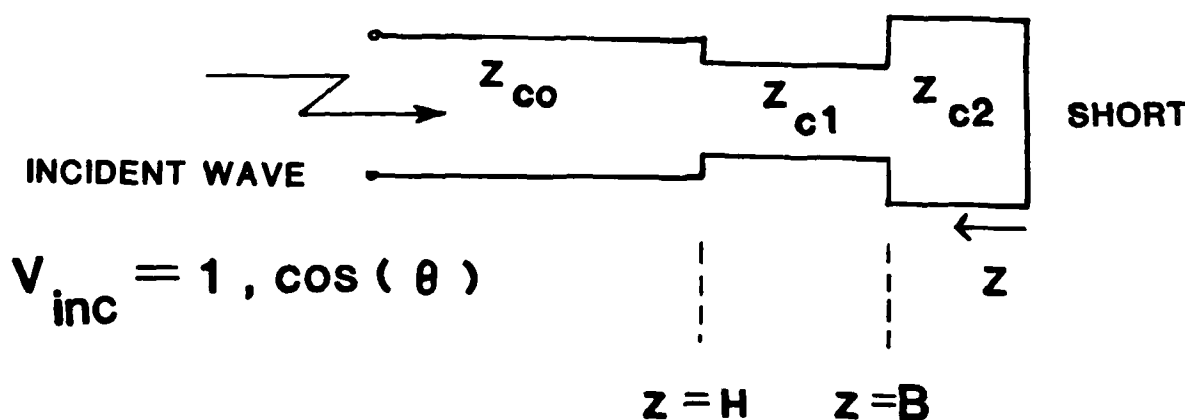
$$Z_{c2} = \eta_o \mu_2 / n_2(\theta)$$

For G(θ)

$$Z_{co} = \eta_o \cos(\theta)$$

$$Z_{c1} = \eta_o n_1(\theta) / \epsilon_1$$

$$Z_{c2} = \eta_o n_2(\theta) / \epsilon_2$$



$$\beta_o = k_o$$

$$\beta_1 = k_o n_1(\theta)$$

$$\beta_2 = k_o n_2(\theta)$$

Figure 2

Transmission Line Analogy

\bar{E} -PLANE PATTERN

$$\epsilon_1 = 2.1$$

$$n_1 B/\lambda_0 = .50$$

$$\mu_1 = 1.0$$

$$n_2 t/\lambda_0 = .25$$

$$\epsilon_2 = 100.0$$

$$z_0/B = .50$$

$$\mu_2 = 1.0$$

$$\text{Gain } (0^\circ) = 21.271 \text{ dB}$$

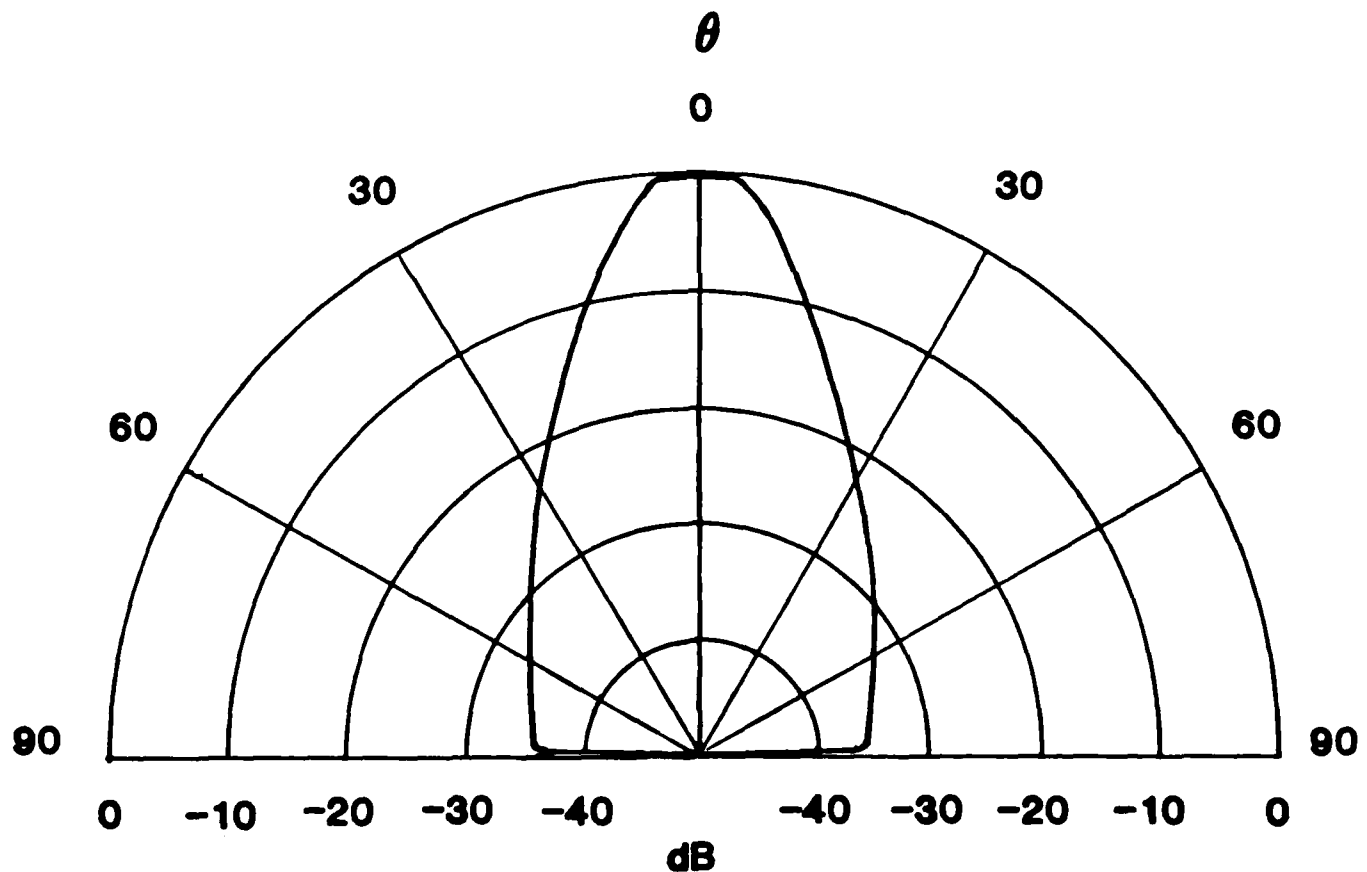


Figure 3a

$\overline{\text{H}}$ -PLANE PATTERN

$$\epsilon_1 = 2.1 \quad n_1 B / \lambda_0 = .50$$

$$\mu_1 = 1.0 \quad n_2 t / \lambda_0 = .25$$

$$\epsilon_2 = 100.0 \quad z_0 / B = .50$$

$$\mu_2 = 1.0$$

$$\text{Gain}(0^\circ) = 21.271 \text{ dB}$$

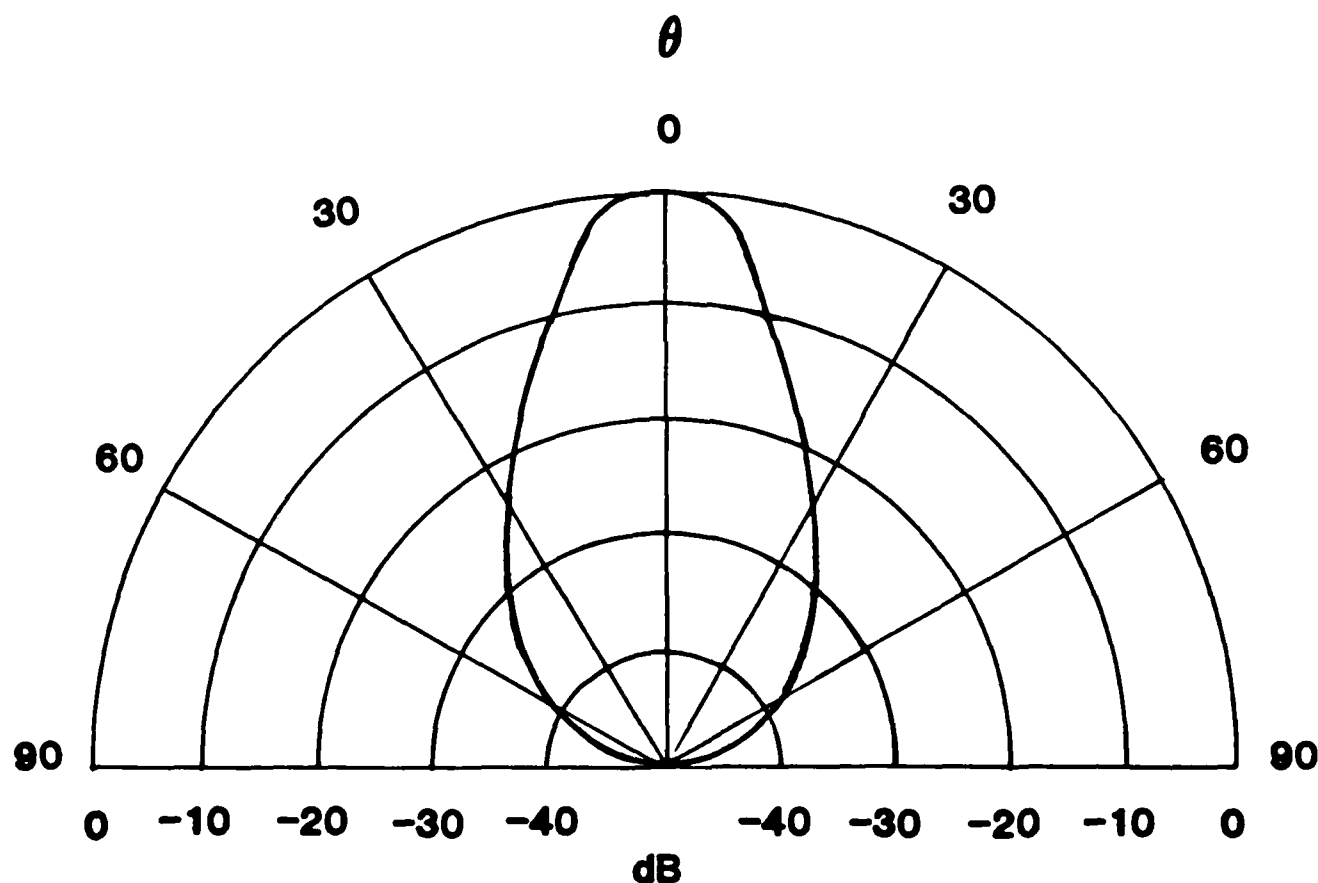


Figure 3b

\bar{E} -PLANE PATTERN

$$\epsilon_1 = 2.1 \quad n_1 B / \lambda_0 = .25$$

$$\mu_1 = 1.0 \quad n_2 t / \lambda_0 = .25$$

$$\epsilon_2 = 1.0 \quad z_0 = B$$

$$\mu_2 = 100.0$$

$$\text{Gain } (0^\circ) = 21.458 \text{ dB}$$

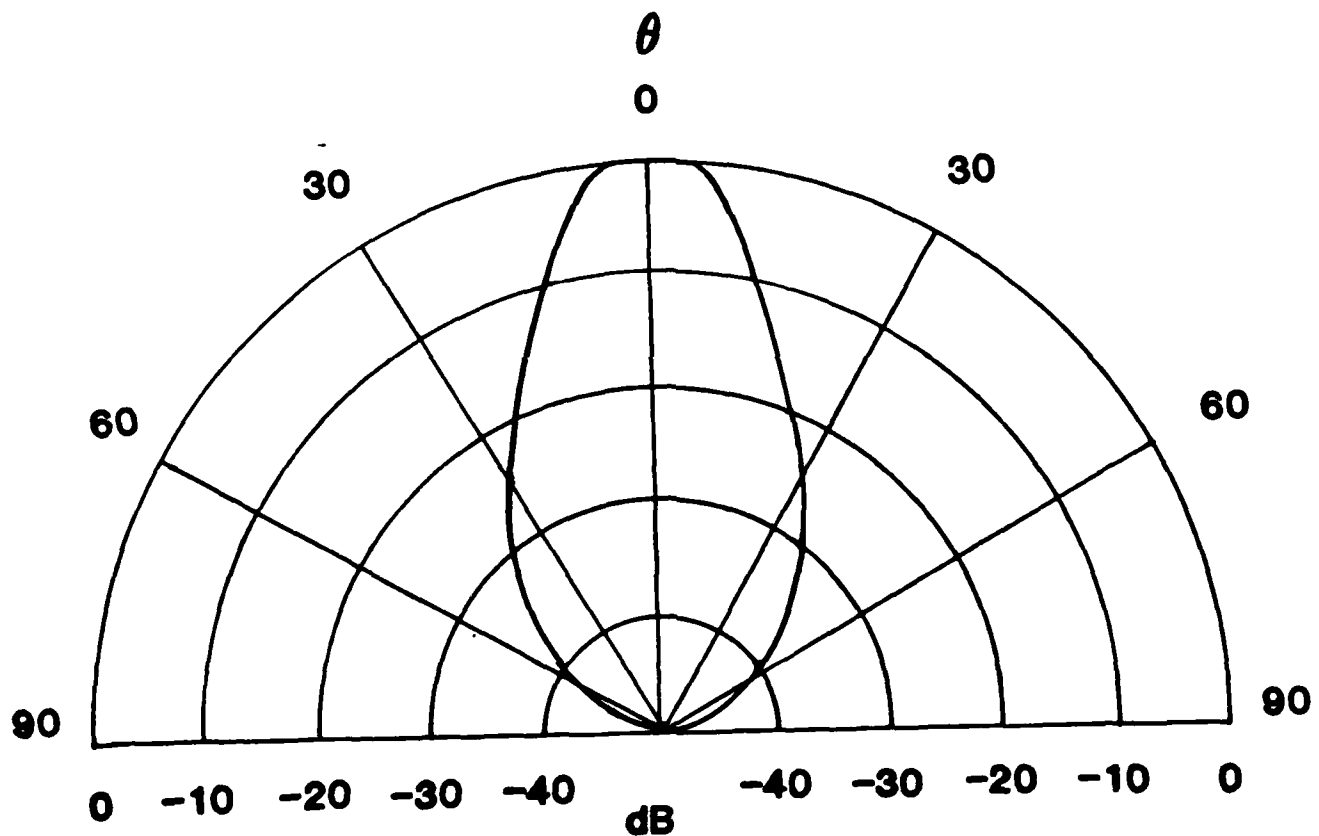


Figure 4a

\overline{H} -PLANE PATTERN

$$\epsilon_1 = 2.1 \quad n_1 B / \lambda_o = .25$$

$$\mu_1 = 1.0 \quad n_2 t / \lambda_o = .25$$

$$\epsilon_2 = 1.0 \quad z_o = B$$

$$\mu_2 = 100.0$$

$$\text{Gain } (0^\circ) = 21.458 \text{ dB}$$

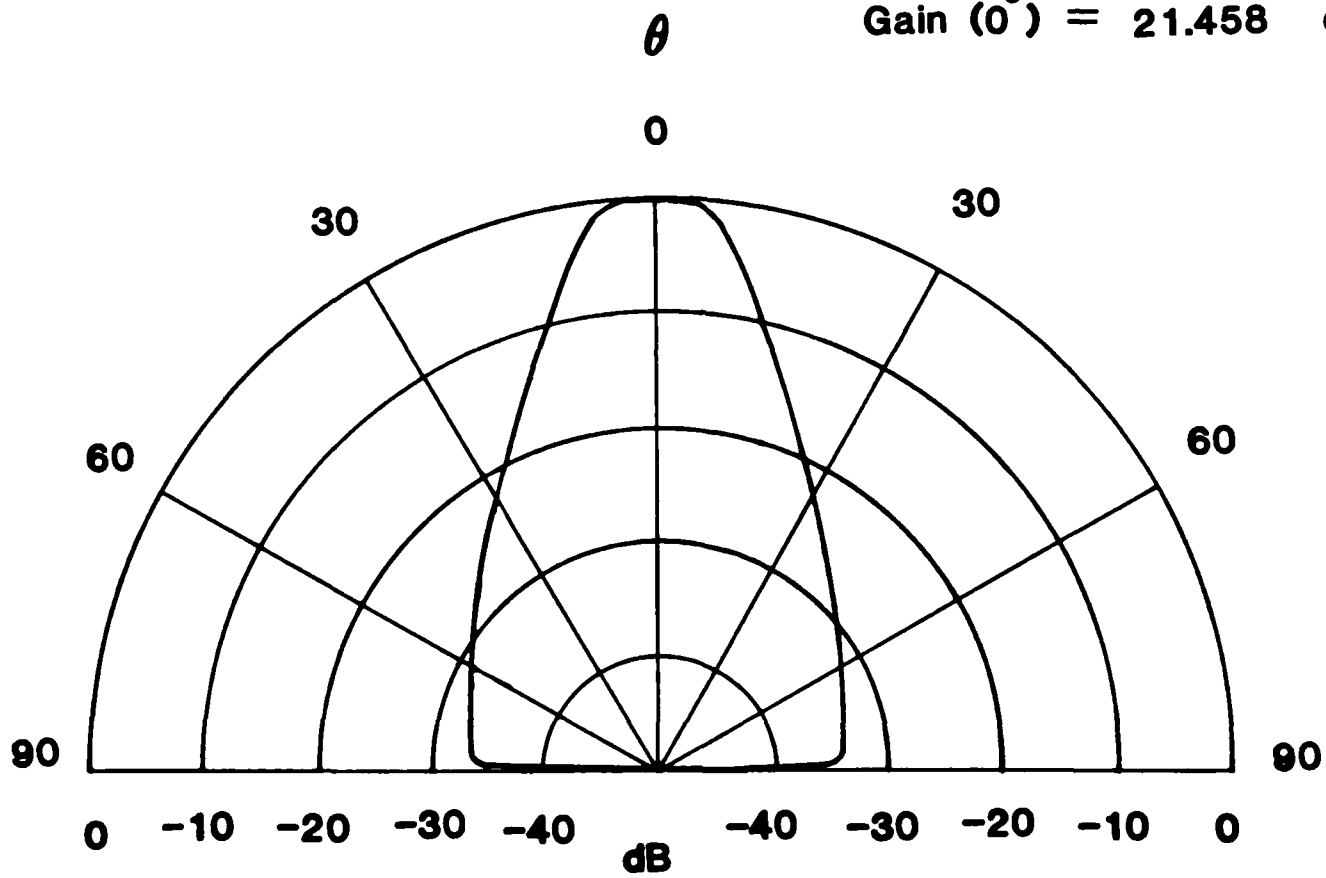


Figure 4b

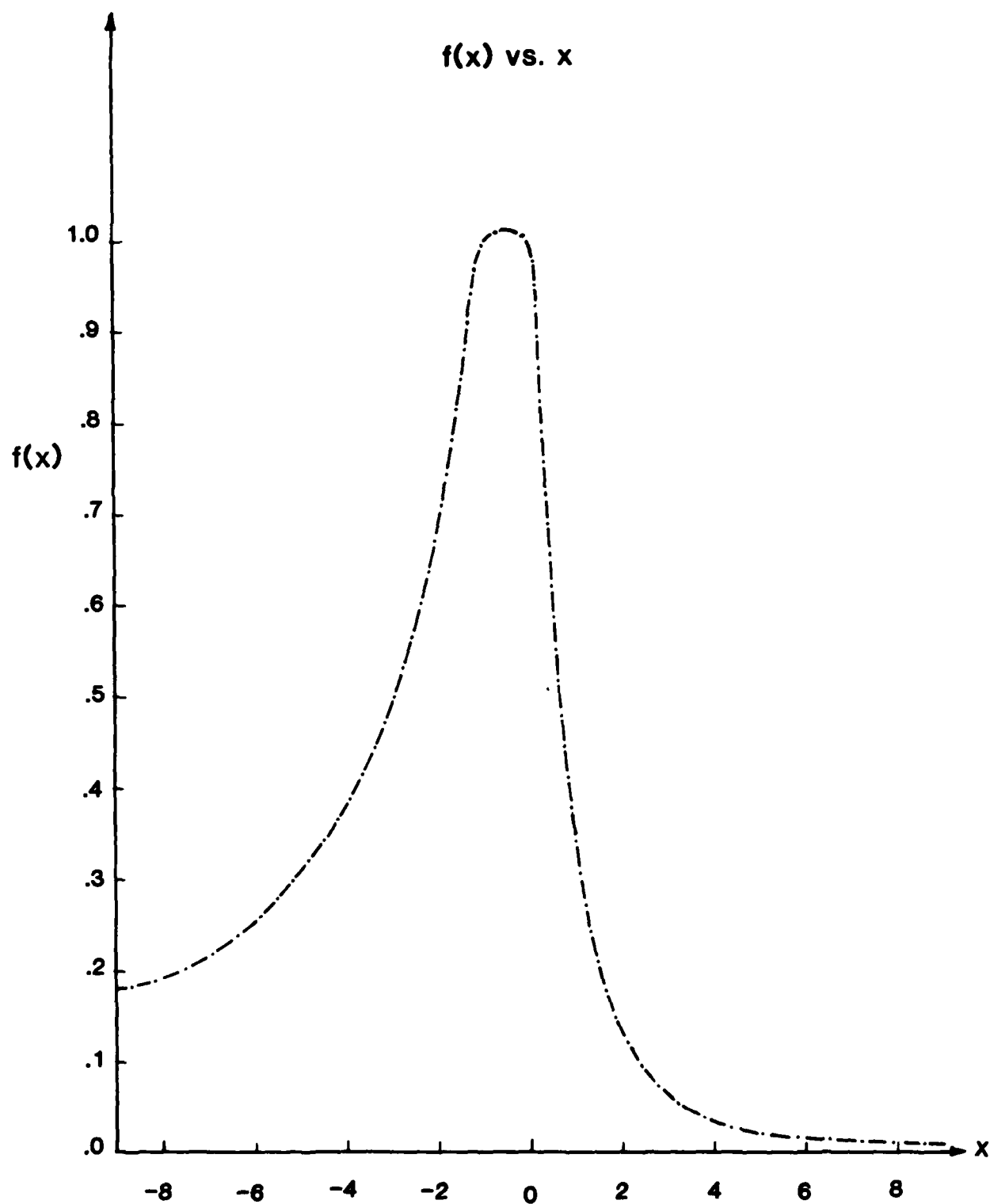


Figure 5

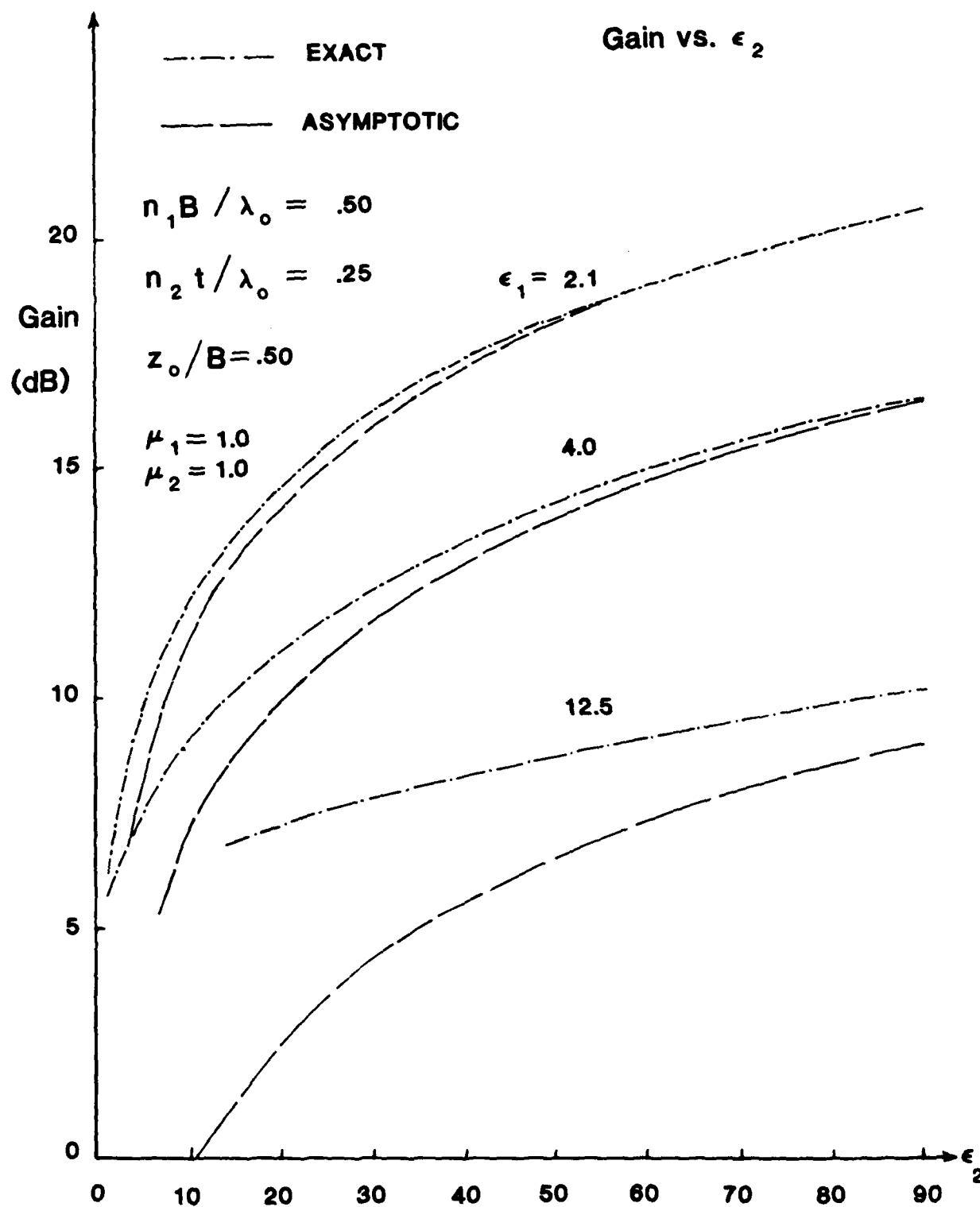


Figure 6a

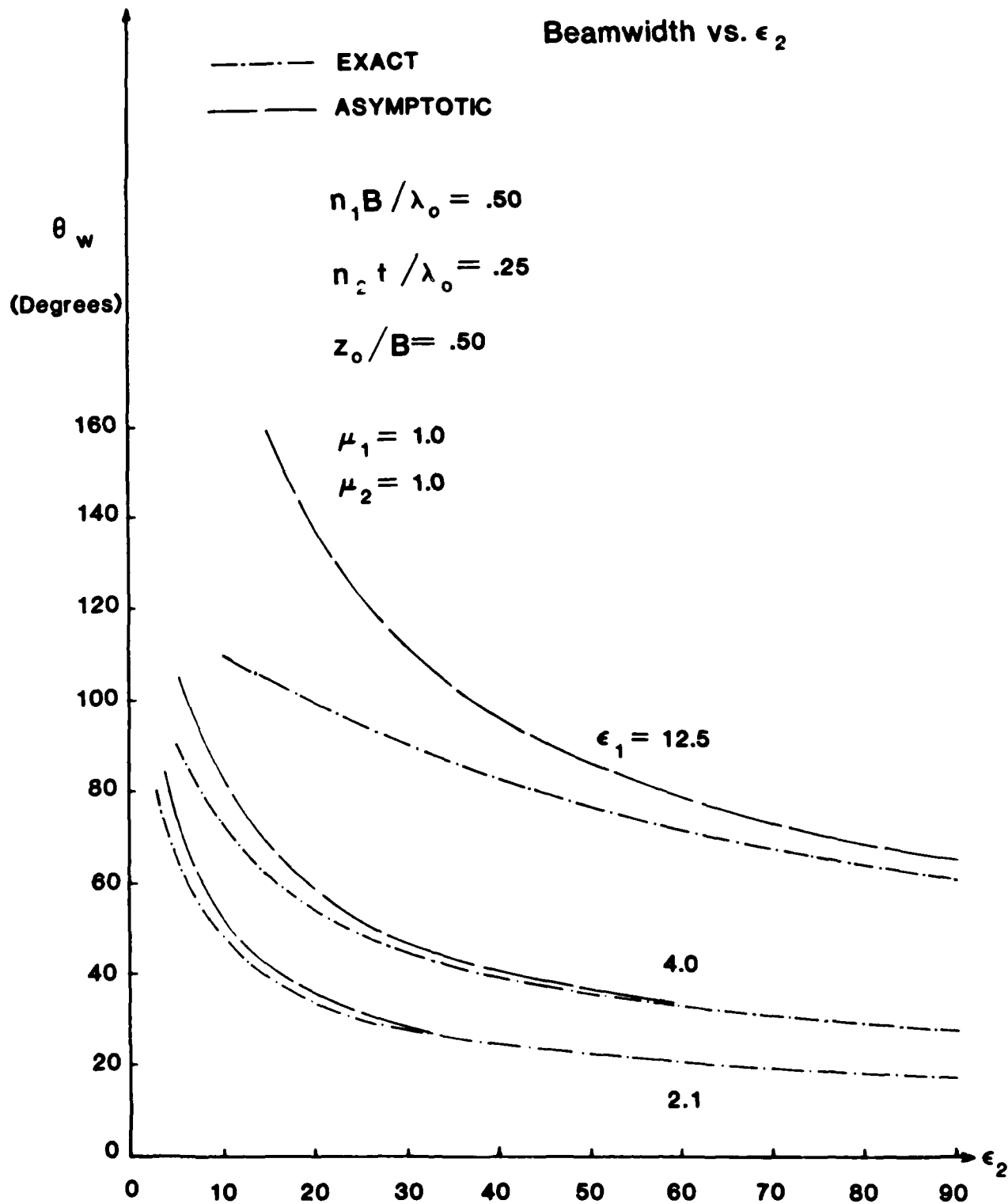


Figure 6b

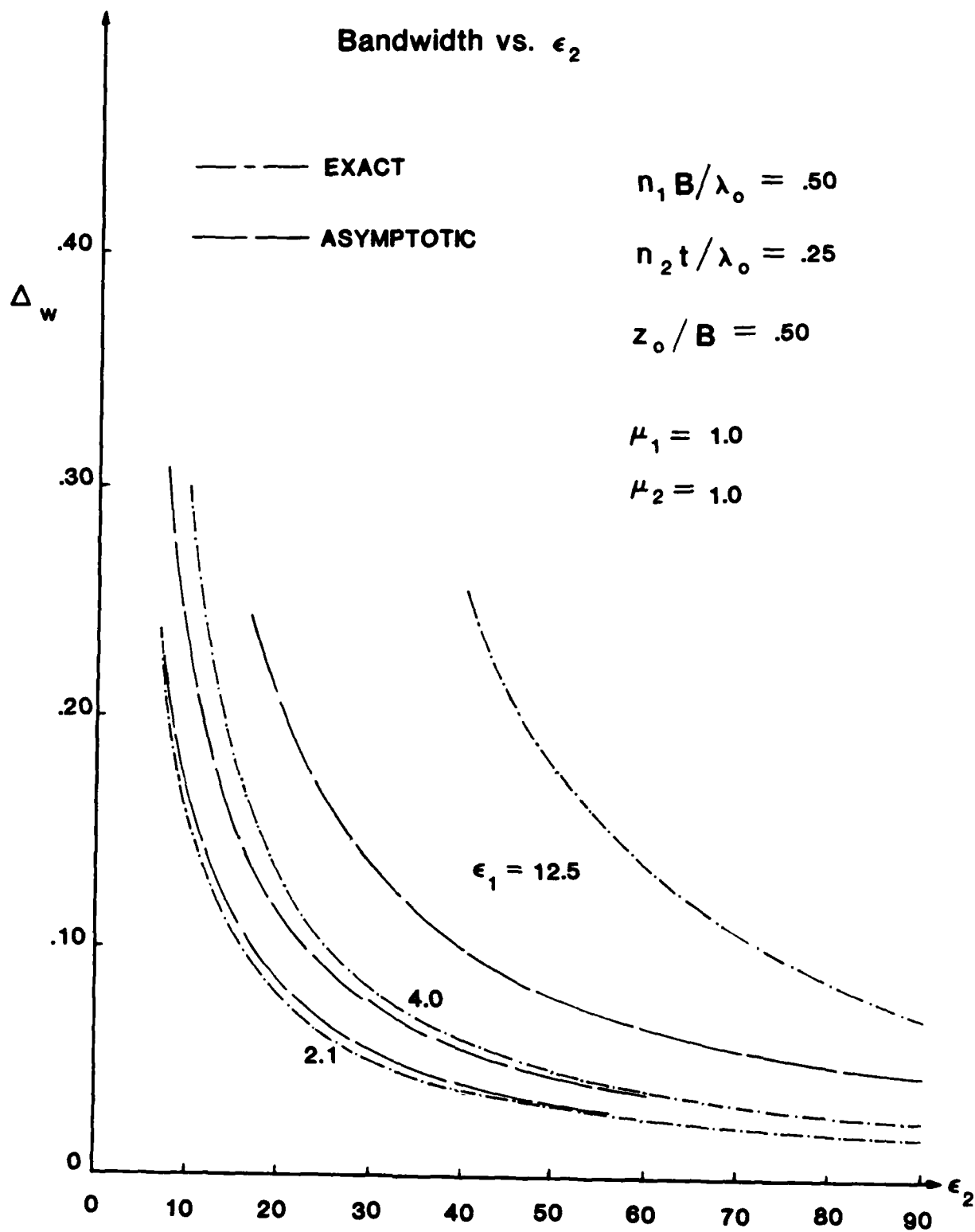


Figure 6c

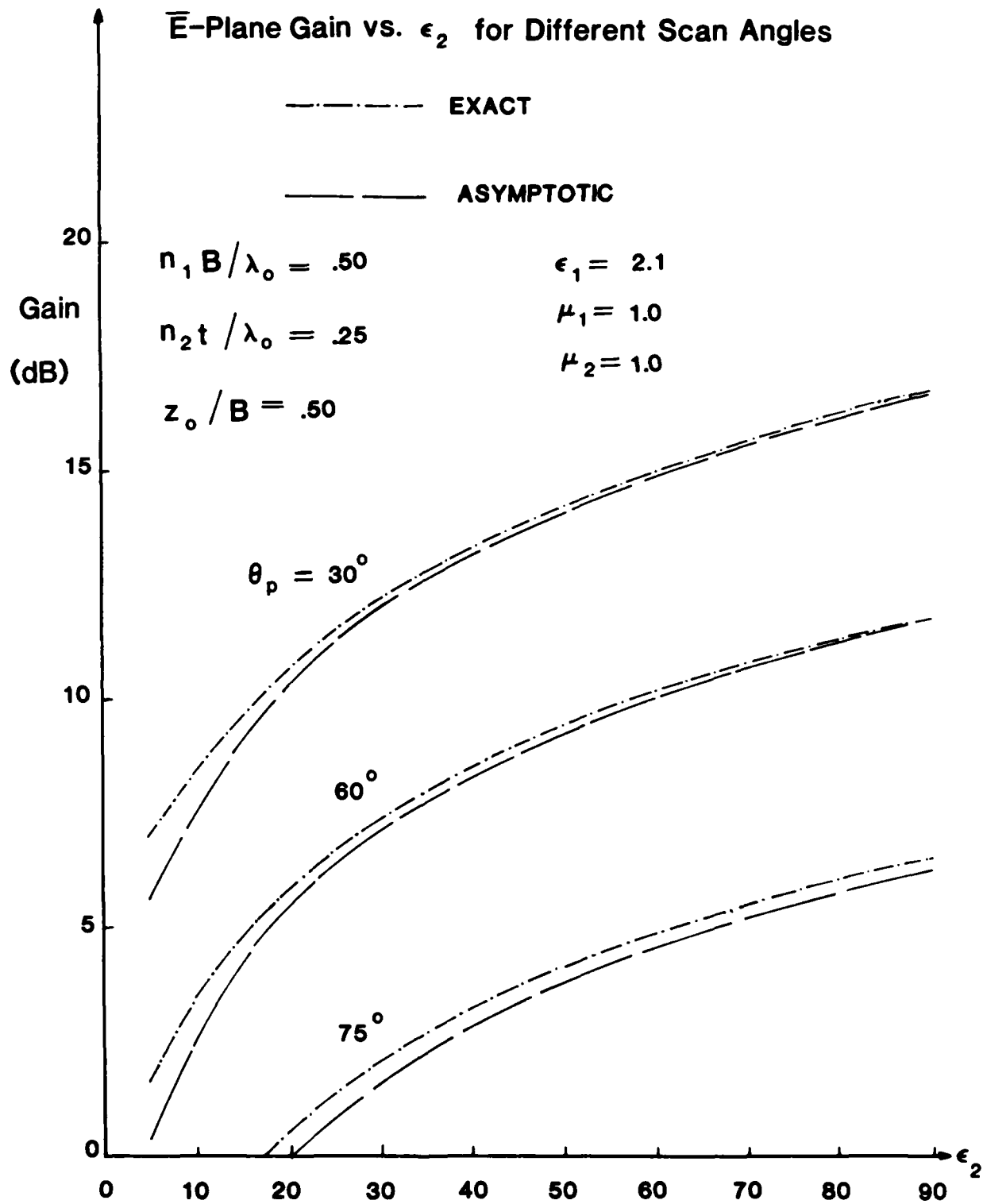


Figure 7a

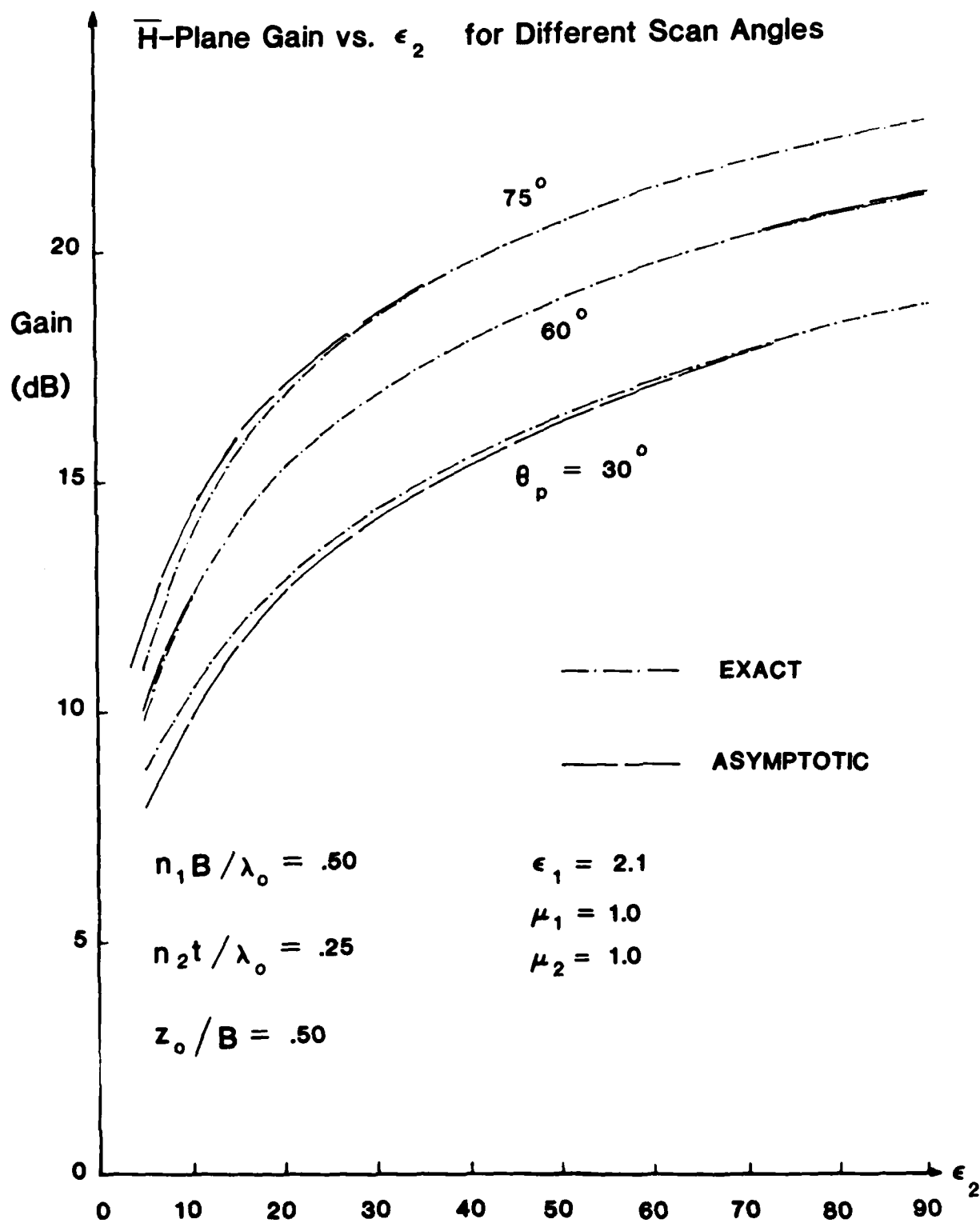


Figure 7b

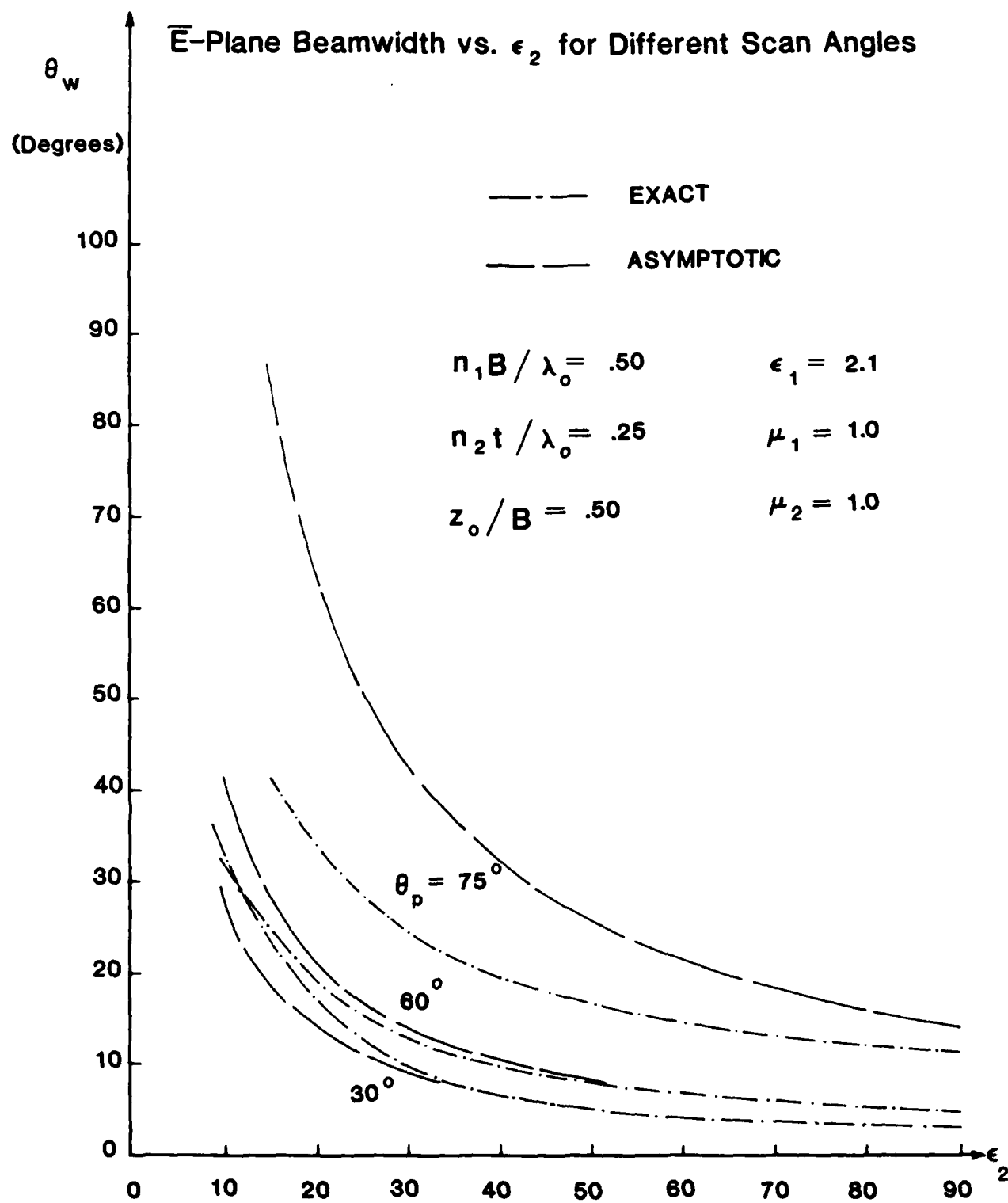


Figure 8a

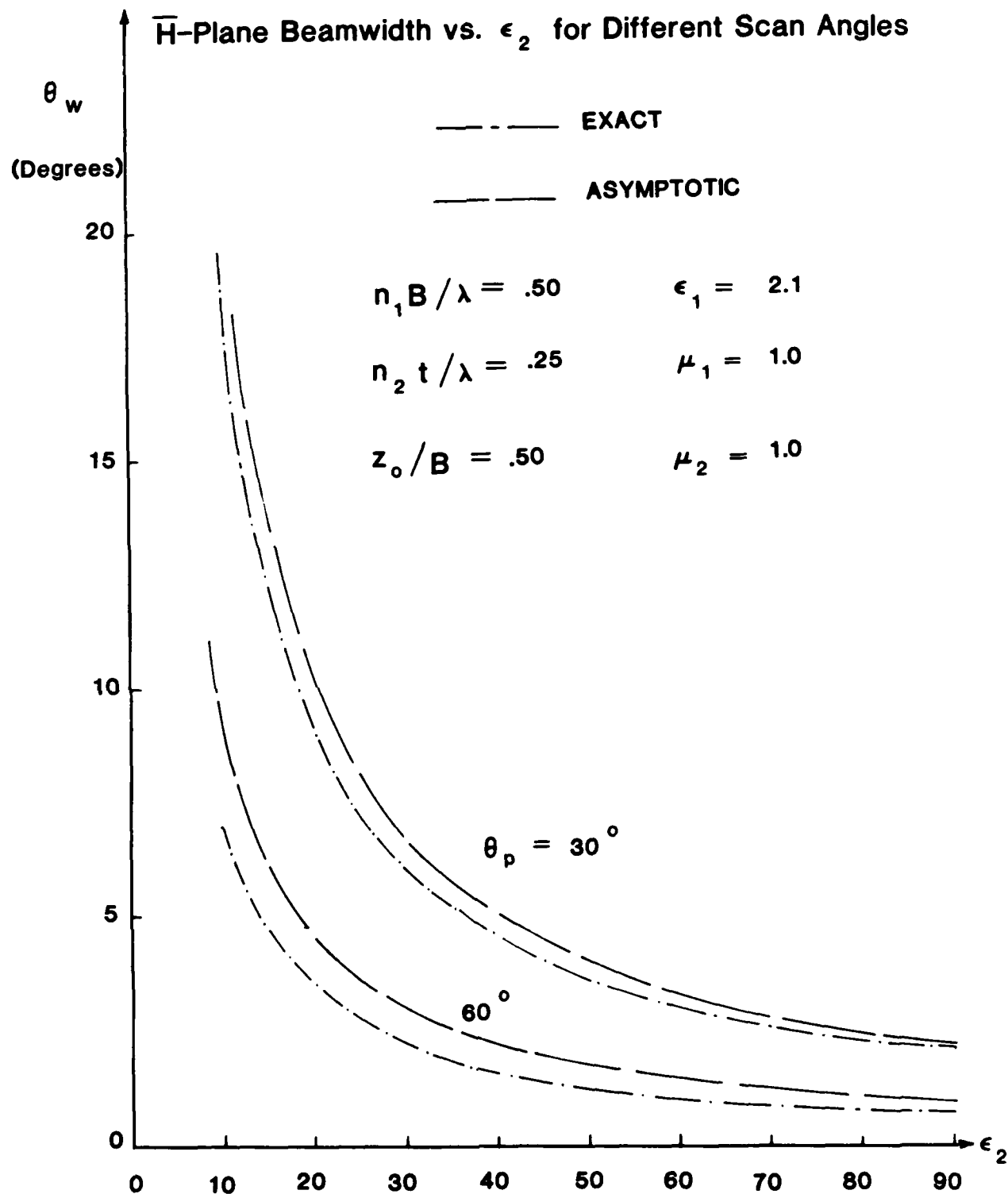


Figure 8b

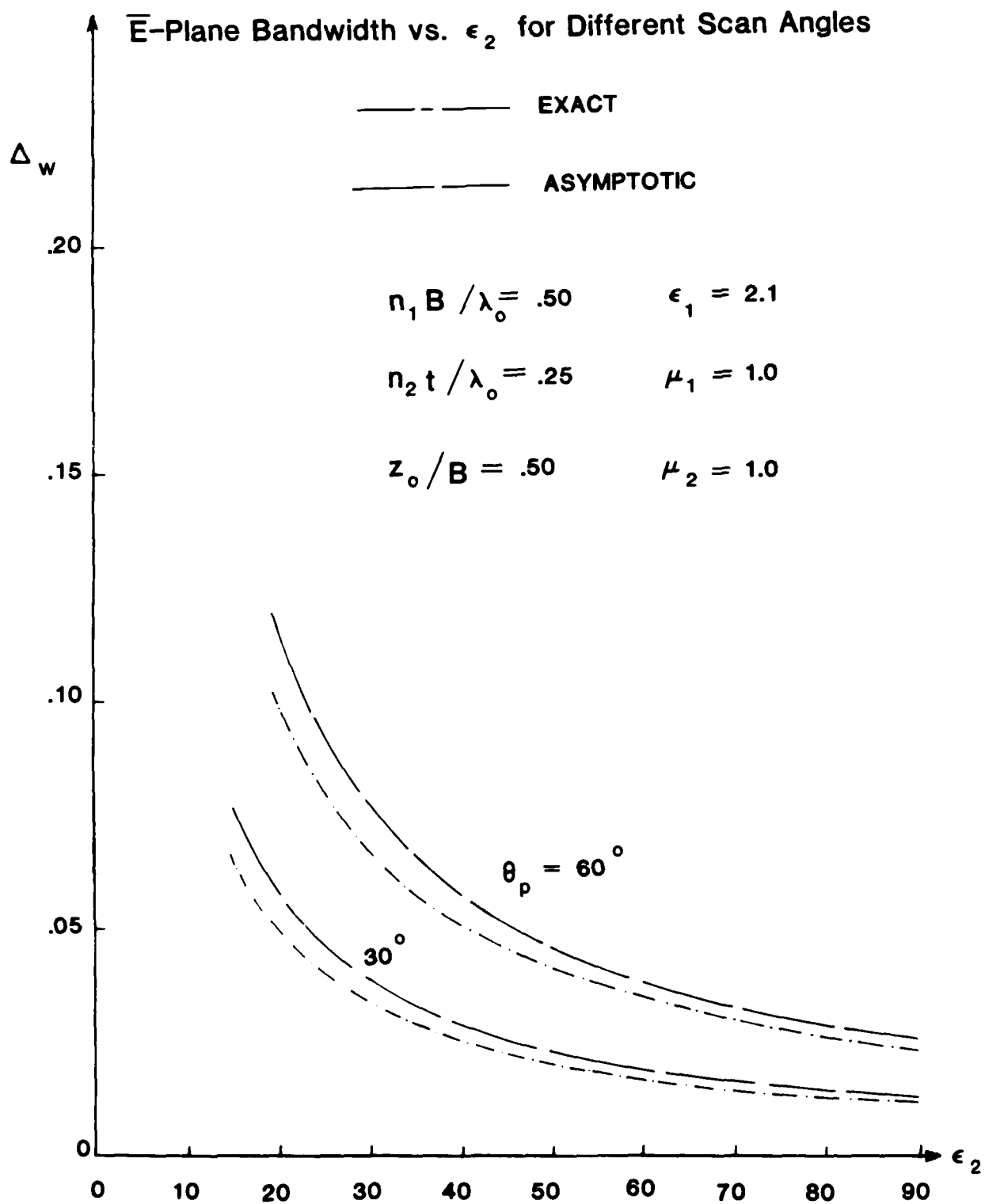


Figure 9a

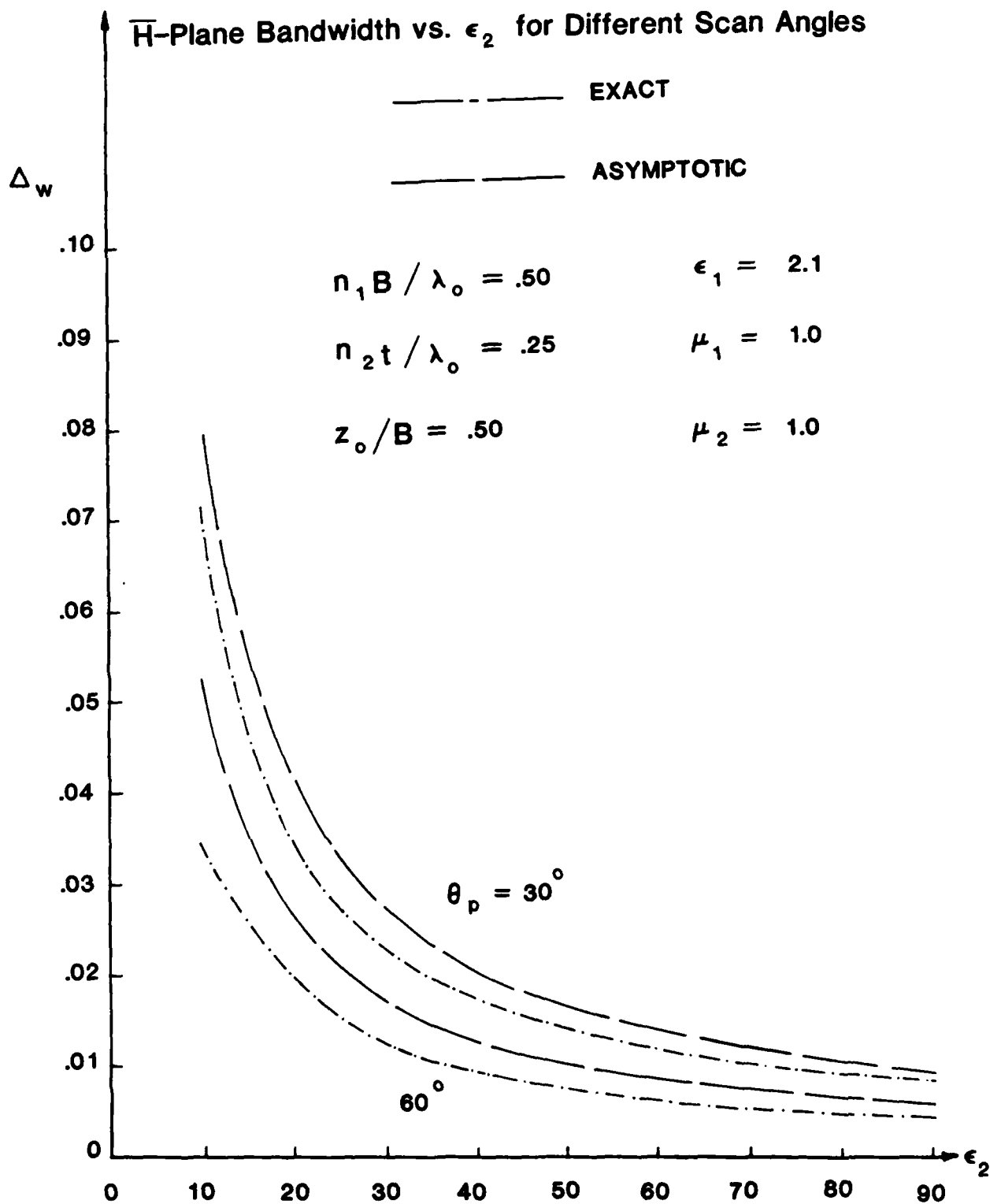


Figure 9b

\overline{E} -PLANE PATTERN

$$\epsilon_1 = 2.1 \quad n_1 B / \lambda_o = .57282$$

$$\mu_1 = 1.0 \quad n_2 t / \lambda_o = .25063$$

$$\epsilon_2 = 100.0 \quad z_o / B = .50$$

$$\mu_2 = 1.0$$

$$\text{Gain } (45^\circ) = 15.21 \text{ dB}$$

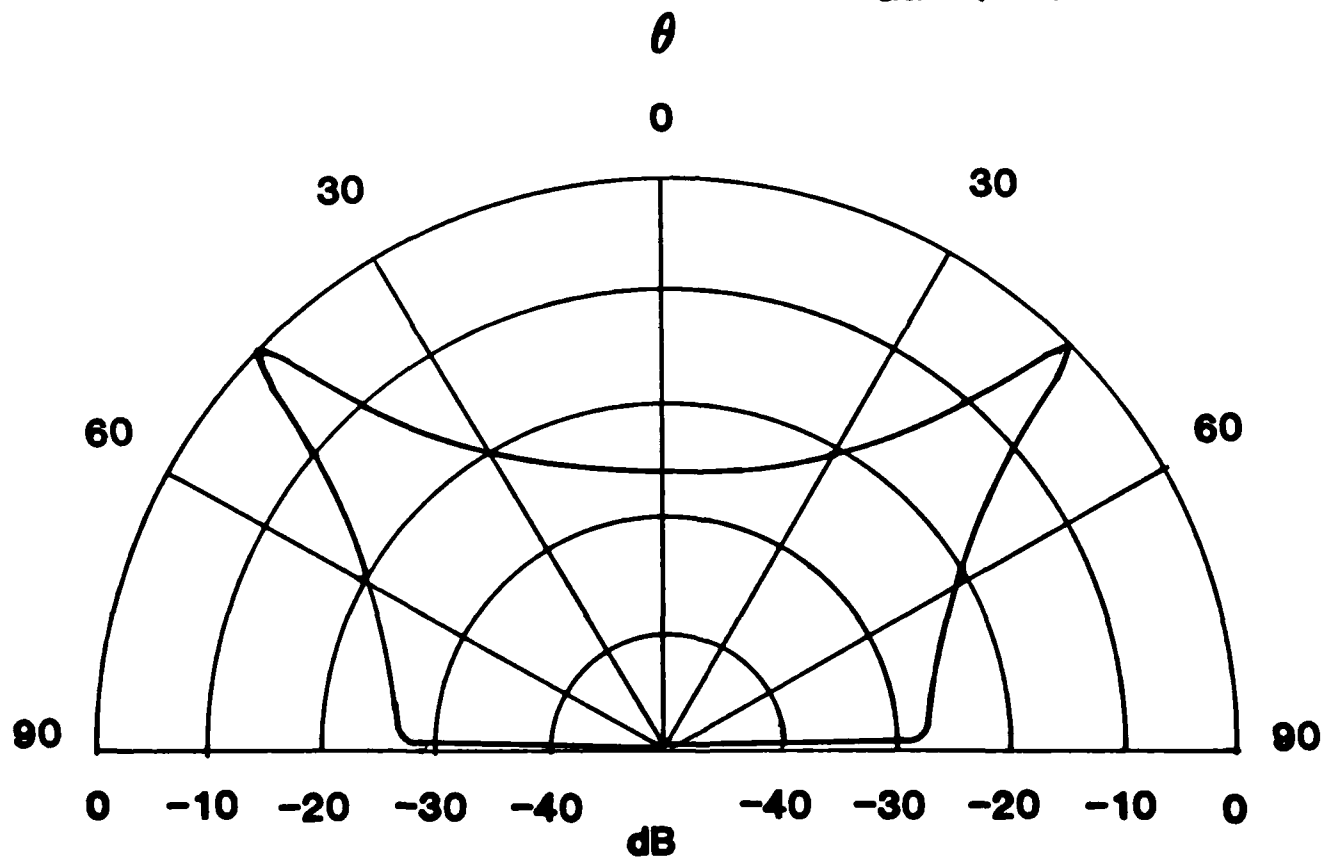


Figure 10a

\bar{H} -PLANE PATTERN

$$\epsilon_1 = 2.1 \quad n_1 B / \lambda_0 = .57282$$

$$\mu_1 = 1.0 \quad n_2 t / \lambda_0 = .25063$$

$$\epsilon_2 = 100.0 \quad z_0 / B = .50$$

$$\mu_2 = 1.0$$

$$\text{Gain } (45^\circ) = 20.54 \text{ dB}$$

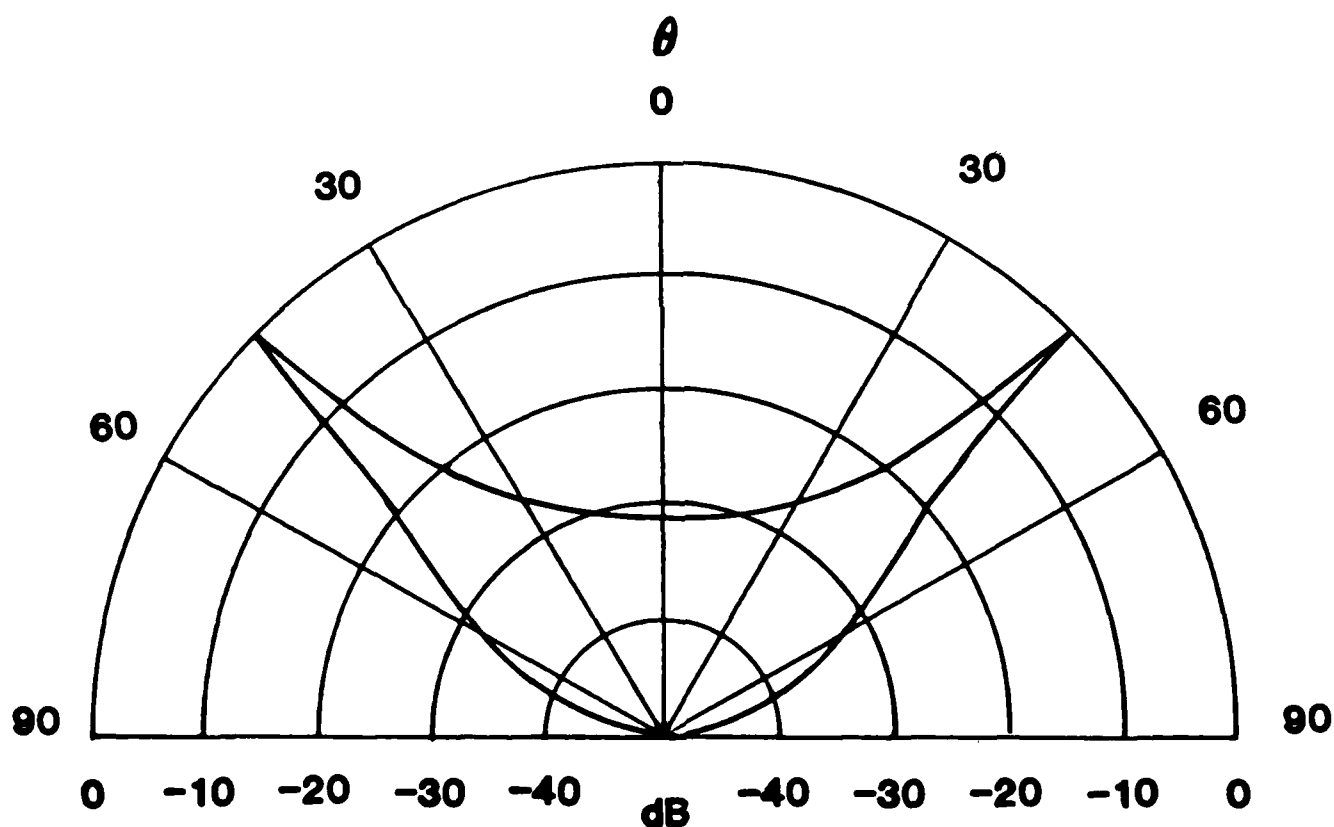


Figure 10b

\overline{H} -PLANE PATTERN

$$\epsilon_1 = 2.1 \quad n_1 B / \lambda_0 = .69085$$

$$\mu_1 = 1.0 \quad n_2 t / \lambda_0 = .25126$$

$$\epsilon_2 = 100.0 \quad z_0 / B = .50$$

$$\mu_2 = 1.0$$

$$\text{Gain } (90^\circ) = 24.64 \text{ dB}$$

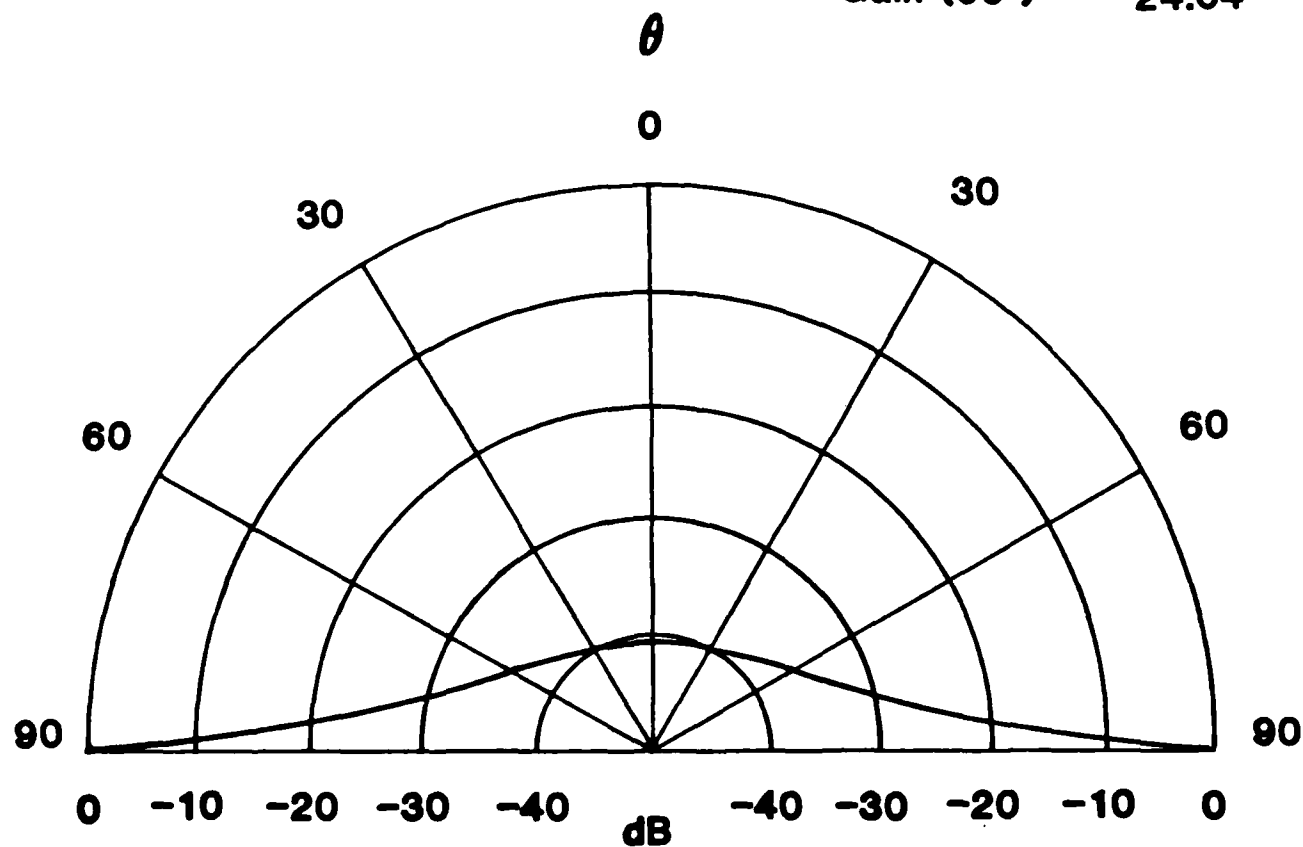


Figure 11a

\overline{E} -PLANE PATTERN

$$\epsilon_1 = 2.1 \quad n_1 B / \lambda_o = .69085$$

$$\mu_1 = 1.0 \quad n_2 t / \lambda_o = .25126$$

$$\epsilon_2 = 100.0 \quad z_o / B = .50$$

$$\mu_2 = 1.0$$

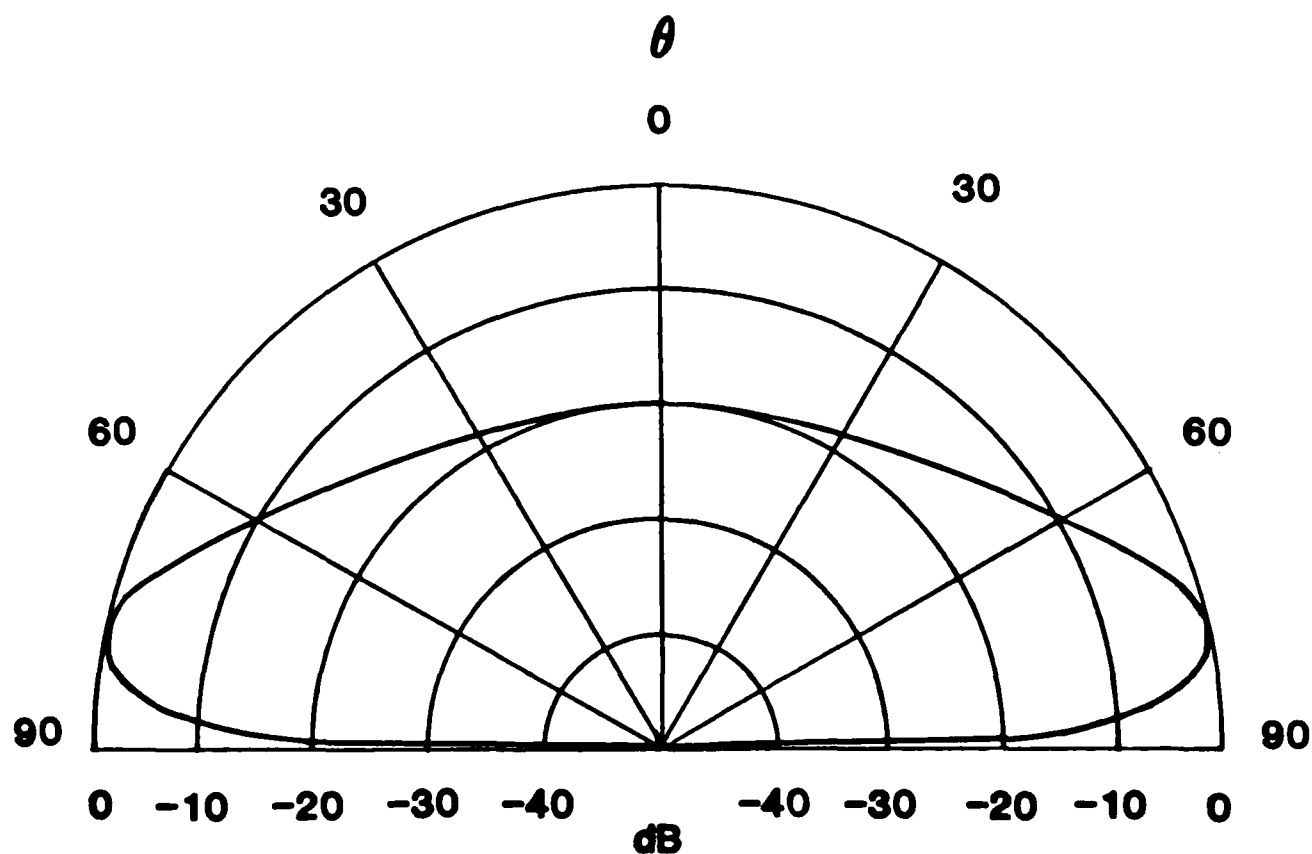


Figure 11b

\overline{E} -PLANE PATTERN

$$\epsilon_1 = 1.23910$$

$$n_1 B / \lambda_0 = 2.79816$$

$$\mu_1 = 1.0$$

$$n_2 t / \lambda_0 = .25$$

$$\epsilon_2 = 25.0$$

$$z_0 / B = .50$$

$$\mu_2 = 1.0$$

$$\text{Gain } (30^\circ) = 19.01 \text{ dB}$$

$$\text{Gain } (70^\circ) = 6.62 \text{ dB}$$

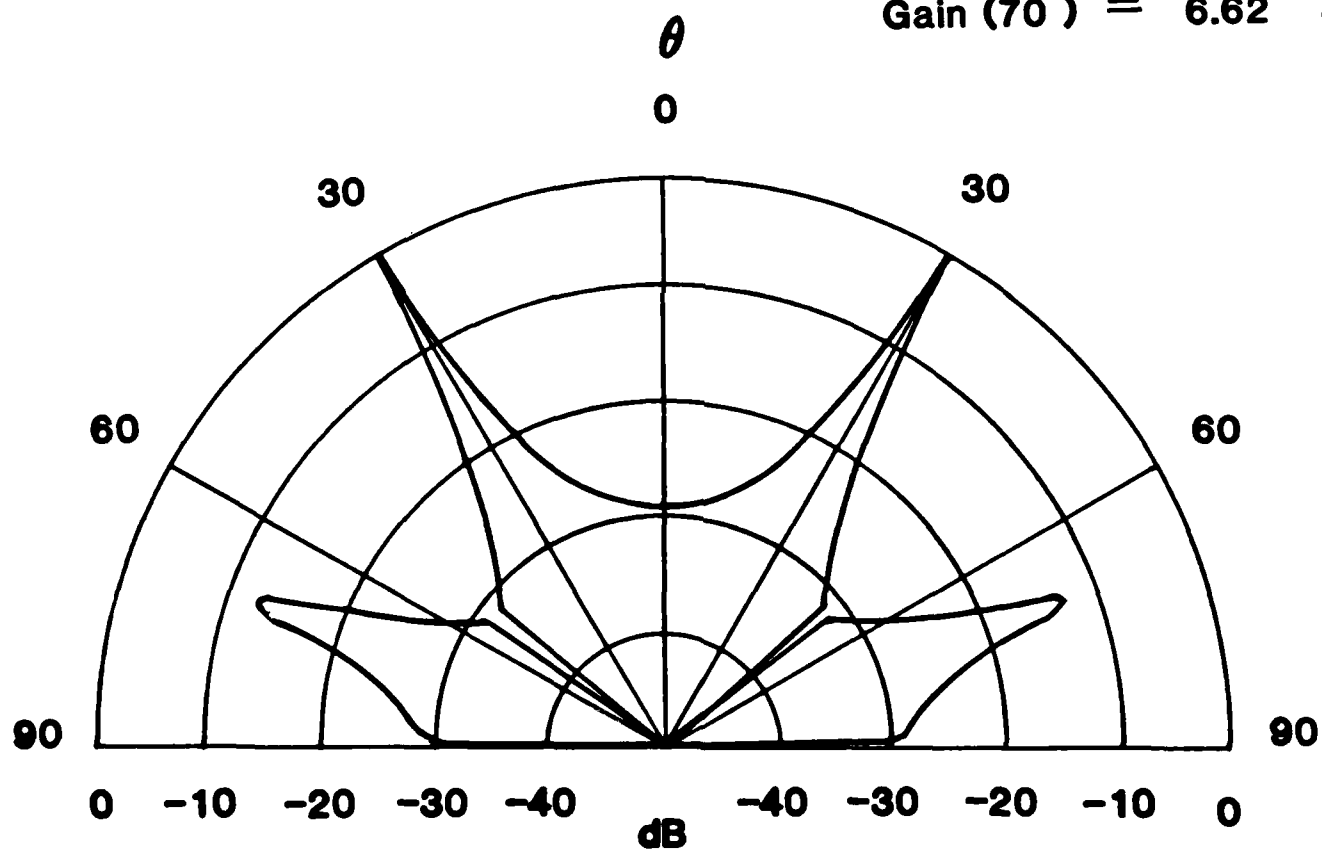


Figure 12a

\bar{H} -PLANE PATTERN

$$\epsilon_1 = 1.23910$$

$$n_1 B / \lambda_0 = 2.79816$$

$$\mu_1 = 1.0$$

$$n_2 t / \lambda_0 = .25$$

$$\epsilon_2 = 25.0$$

$$z_0 / B = .50$$

$$\mu_2 = 1.0$$

$$\text{Gain } (30^\circ) = 22.13 \text{ dB}$$

$$\text{Gain } (70^\circ) = 26.46 \text{ dB}$$

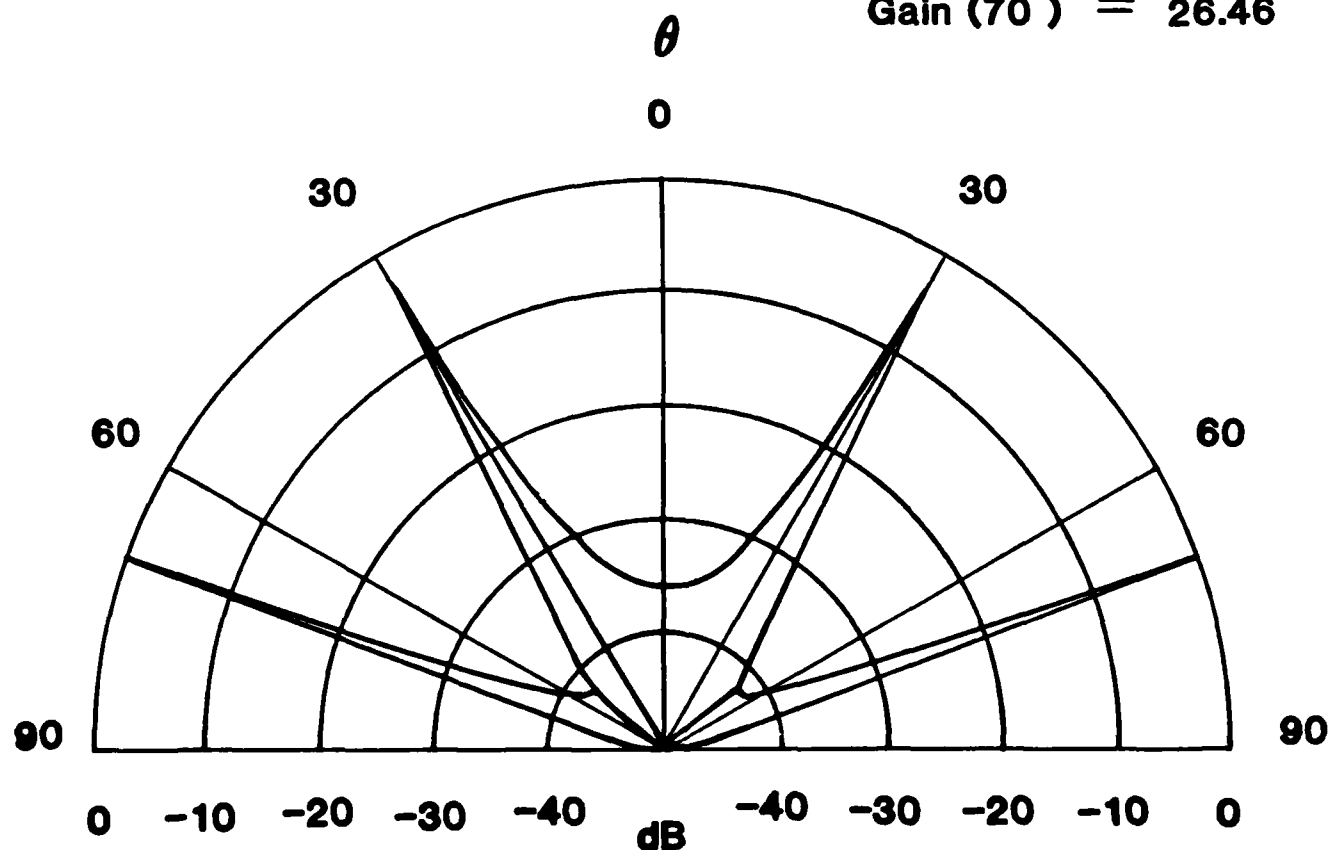


Figure 12b

END

FILMED

3-85

DTIC